

# van der Waals forces in presence of free charges: An exact derivation from equilibrium quantum correlations

A. Alastuey

*Laboratoire de Physique, UMR 5672 du CNRS, ENS Lyon, 46 allée d'Italie, F-69364 Lyon Cedex 07, France*

F. Cornu

*Laboratoire de Physique Théorique, UMR 8627 du CNRS, Université Paris-Sud, Bâtiment 210, F-91405 Orsay, France*

Ph. A. Martin

*Institute of Theoretical Physics, Swiss Federal Institute for Technology Lausanne, CH-1015, Lausanne EPFL, Switzerland*

(Received 27 February 2007; accepted 4 June 2007; published online 3 August 2007)

We study interatomic forces in a fluid consisting of a mixture of free charges and neutral atoms in the framework of the quantum many-body problem at nonzero temperature and nonzero density. Of central interest is the interplay between van der Waals forces and screening effects due to free charges. The analysis is carried out in a partially recombined hydrogen plasma in the Saha regime. The effective potentials in the medium between two atoms, or an atom and a charge, or two charges, are determined from the large-distance behavior of equilibrium proton-proton correlations. We show, in a proper low-temperature and low-density scaling limit, that those potentials all decay as  $r^{-6}$  at large distance  $r$ , while the corresponding amplitudes are calculated exactly. In particular, the presence of free charges only causes a partial (nonexponential) screening of the atomic potential, and it does not modify its typical  $r^{-6}$  decay. That potential reduces to the standard van der Waals form for two atoms in vacuum when the temperature is driven to zero. The analysis is based on first principles: it does not assume preformed atoms and takes into account in a coherent way all effects, quantum mechanical binding, ionization, and collective screening, which originate from the Coulomb potential. Our method relies on the path integral representation of the quantum Coulomb gas. © 2007 American Institute of Physics. [DOI: [10.1063/1.2753146](https://doi.org/10.1063/1.2753146)]

## I. INTRODUCTION

### A. Motivation

The existence of van der Waals attraction between atoms and molecules is at the origin of a broad variety of phenomena ranging from condensation of liquids and cohesion of solids to structure effects in colloid chemistry and biology (see, e.g., Refs. 1 and 2). van der Waals attraction between two atoms in their ground states in the vacuum arises from electromagnetic interactions generated by their instantaneous electrical dipoles. At not too large separations, both retardation effects and magnetic forces can be neglected, so only Coulomb interactions have to be retained. Then, the resulting effective interaction at distances large compared to the Bohr radius can be computed within the familiar perturbation theory, since the dipole-dipole Coulomb interaction between the two atoms is negligible with respect to the atomic binding energies (London calculation). For atoms which carry no permanent dipoles, the averaged electrical dipoles vanish and, according to second order perturbation theory, their quantum fluctuations give rise to a squared dipolar effective interaction (see, e.g., Ref. 3). In the most elementary theory of fluids, that effective interaction is introduced phenomenologically in a statistical mechanical description of the system, where atoms are now treated as preformed entities (the so-

called chemical picture): atoms are assumed to interact *via* a two-body potential, the attractive long-range part of which precisely reduces to above van der Waals interactions.

When the atoms or molecules interact across an intervening medium (e.g., a solvent), the calculation of van der Waals forces resorts to the theory of electromagnetic fluctuations in the medium.<sup>4,5</sup> The amplitude of the van der Waals potential is then expressed as a sum over imaginary frequencies (Matsubara frequencies) of products of individual atomic polarizabilities. The latter embody the influence of the medium and have to be determined from experimental data on absorption spectra or from suitable models for the response functions. This amounts to treat solvent effects within linear response theory. The corresponding modified van der Waals forces can be also retrieved via a suitable adaptation of Lifchitz and Pitaevskii theory<sup>6</sup> for the forces between macroscopic bodies.

If free charges are present in the medium (e.g., provided by the dissolution of a salt in an electrolyte, or by thermal or pressure ionization in a gas), van der Waals forces will be altered because of screening. One usually assumes at this point (Ref. 5, Chap. 7) that the zero frequency (static) term of the polarizability is modified according to the classical Debye-Hückel theory of screening, but the nonzero frequency terms remain essentially unaffected by the presence

of free charges because of the inability for cations and anions to follow rapid oscillatory motion. In this way the long-range  $1/r^6$  tail of the intermolecular potential is supposed to survive exponential static screening. In fact, the Derjaguin, Landau, Verwey, Overbeek (DVLO) theory is precisely about stabilizing colloidal dispersions by screened electrostatic repulsion against the remaining attractive van der Waals forces that would otherwise lead to flocculation.<sup>4,7</sup> At a quantitative level, weakening of van der Waals attraction by free charges has been assumed to be small (and even negligible) in numerous theoretical works. However, that effect may become rather important in some situations, as shown by a recent experiment about the swelling of phospholipids in presence of highly concentrated monovalent salt.<sup>8</sup>

If above arguments about weakening of van der Waals forces by free charges are physically sound, the corresponding calculations involve uncontrolled approximations and guesses, which are rather questionable. Use of linear response may be unappropriate since the electromagnetic fields created by perturbing sources (the atoms) are not infinitesimal quantities. Static and dynamic aspects of screening are arbitrarily separated, without a detailed analysis of the physical conditions under which such separation might be valid. For instance, the argument about slow inertial motion of charges which prevents screening of the nonzero frequency part of the atomic susceptibility is not supported by any estimation of the influence of their masses.

The main purpose of this paper is to propose a consistent scheme for deriving van der Waals forces at finite temperature and finite density, within the framework of equilibrium statistical mechanics. Then, effective potentials will be defined from equilibrium particle correlations. In that context, the quantum nature of electrons and nuclei cannot be ignored, since it is at the very origin of van der Waals forces. Moreover, quantum mechanical screening does incorporate dynamical features<sup>9</sup> which are also crucial. As it is well known, equilibrium properties of a quantum system are not determined by a static configurational integral like in the classical case. On the contrary, they always keep trace of dynamical effects, since both static and dynamical contributions remain entangled. As far as screening is concerned, this implies that the effective potential between two quantum point charges decays only as  $1/r^6$  in general, even when the surrounding plasma is purely classical. That algebraic tail originates from the quantum fluctuations of charge positions, irrespective of the fact that they are free or bound in atoms or molecules.

This fundamental aspect of quantum mechanical screening is best understood in the Feynman path integral representation of Coulomb fluids, which will be used throughout this paper. Since this formalism is perhaps not so familiar to the reader, it is worth to qualitatively describe here the mechanism which is at the source of the loss of the standard classical exponential Debye screening. In the path integral representation, a quantum point charge appears as an extended object, consisting of a random charged filament (like a tiny charged wire) associated with the intrinsic quantum fluctuation of the particle. In this language, the underlying dynamical effects are precisely materialized by the fluctuations of

those filaments. One conceives that two quantum charges, in addition to the  $r^{-1}$  Coulomb potential, are also subjected to multipolar interactions as would experience any nonspherical charge distributions. It turns out that instantaneous dipoles associated with quantum fluctuations cannot be perfectly screened by the polarization clouds, in qualitative agreement with the heuristic findings described above. We emphasize again that such effect is proper to quantum mechanics, irrespective of the actual state, bound or free, of a charge in a medium. If a charge is bound in an atom, its quantum position fluctuations are of the order of the Bohr radius, i.e., the typical atomic size. For a free charge, such fluctuations are of the order of the de Broglie thermal wavelength. We refer the reader to the paper<sup>9</sup> and the reviews<sup>10,11</sup> for a more detailed analysis of the breaking of exponential screening in quantum mechanics (see, in particular, the simple model involving only two particles in Sec. VIII of Ref. 9 and in Sec. IV C of Ref. 11). The dynamical character of quantum screening just described is not captured by mean-field approaches, such as the random phase approximation or Debye-Hückel theory, which predict an exponential decay of the effective potential between charges.<sup>12,13</sup> In some sense, that failure has been anticipated, at least at a qualitative level, in the previous phenomenological methods where exponential screening is only applied to the static part of the considered interactions.

As argued above, our scheme for computing van der Waals forces requires the introduction of the full quantum mechanical many-body problem (the physical picture) so that collective screening due to individual point charges together with formation of atoms and interatomic interactions can be treated simultaneously. For the sake of simplicity, we study the quantum hydrogen plasma made of nonrelativistic protons and electrons with Fermi statistics. That system is described by the basic many-body Coulomb Hamiltonian

$$H_{N_p, N_e} = \sum_{j=1}^{N_p} \frac{|\mathbf{p}_j|^2}{2m_{\alpha_j}} + \sum_{i < j} \frac{e_{\alpha_i} e_{\alpha_j}}{|\mathbf{r}_i - \mathbf{r}_j|} \quad (1.1)$$

for  $N_p$  protons and  $N_e$  electrons ( $N_p + N_e = N$ ) with species index  $\alpha = p, e$ , charges  $e = e_p = -e_e$ , and masses  $m_p, m_e$ . The Hamiltonian (1.1) does not involve the coupling with the electromagnetic field: retardation effects are not considered in this paper. In spite of its apparent simplicity, that system displays a very rich phase diagram in the temperature-density plane. Here we will consider the Saha regime when the system consists in a mixture of hydrogen atoms and ionized protons and electrons. In that regime, exact asymptotic calculations can be performed, which illustrate in depth the interplay between screening and van der Waals forces. We stress that all the effects stemming from the Coulomb interaction, namely, recombination, screening, and effective forces, are dealt with in a systematic and consistent manner.<sup>14</sup>

Our main results are presented in Sec. I B. Their qualitative features are briefly discussed. A detailed comparison to the predictions of previous existing approaches is postponed to another paper. Also, applications of our scheme to other systems where free charges are almost classical ions (like in an electrolyte) will be presented elsewhere.

## B. Statement of the results

First for further comparison, we recall the standard formula for the van der Waals interaction between two hydrogen atoms in their ground states in vacuum. Usually, it is assumed that protons have infinite masses and they are located at fixed positions  $\mathbf{r}_a$  and  $\mathbf{r}_b$ . Then, the atom-atom Coulomb interaction  $V^{\text{at-at}}$  behaves as a dipolar potential at large atomic separation  $|\mathbf{r}| \rightarrow \infty$  with  $\mathbf{r} = \mathbf{r}_a - \mathbf{r}_b$ ,

$$V^{\text{at-at}} \sim \frac{D^{\text{at-at}}}{r^3}, \quad D^{\text{at-at}} = e^2 [\mathbf{y}^{(a)} \cdot \mathbf{y}^{(b)} - 3(\mathbf{y}^{(a)} \cdot \hat{\mathbf{r}})(\mathbf{y}^{(b)} \cdot \hat{\mathbf{r}})], \quad (1.2)$$

where  $\mathbf{y}^{(a,b)}$  is the relative position of the proton and the electron in each atom  $a$  or  $b$ ,  $\mathbf{y}^{(a,b)} = \mathbf{r}_p^{(a,b)} - \mathbf{r}_e^{(a,b)}$  ( $\mathbf{r}_p^{(a,b)} = \mathbf{r}_{a,b}$ ), and  $\hat{\mathbf{r}} = \mathbf{r}/r$ . The van der Waals potential  $U_{\text{vdW}}(r)$ , obtained by treating  $V^{\text{at-at}}$  within perturbation theory up to second order,<sup>3</sup> reads  $U_{\text{vdW}}(r) = C_{\text{vdW}}/r^6$  with the negative constant

$$C_{\text{vdW}} = - \sum_{p_a \neq 0, p_b \neq 0} \frac{|\langle \psi_0^{(a)} \otimes \psi_0^{(b)} | D^{\text{at-at}} | \psi_{p_a}^{(a)} \otimes \psi_{p_b}^{(b)} \rangle|^2}{E_{p_a} + E_{p_b} - 2E_0}. \quad (1.3)$$

In Eq. (1.3), index  $p$  is a collective notation for the quantum numbers which determine the (internal) eigenwave function  $\psi_p(\mathbf{y})$  of a single atom with energy  $E_p$ , while  $p=0$  defines the ground state  $\psi_0(y)$  with energy  $E_0$ . The sum runs over all excited states  $\psi_{p_a}^{(a)} \otimes \psi_{p_b}^{(b)}$ ,  $(p_a, p_b) \neq (0, 0)$ , of the two atoms (the notation includes the integral over the continuous part of the spectrum). As checked further, the assumption of infinitely heavy protons can be relaxed by using in Eq. (1.3) the reduced mass  $m = m_p m_e / (m_p + m_e)$  for computing  $\psi_p(\mathbf{y})$  and  $E_p$  (contributions of atom mass centers do not intervene here). Then, ground state energy is  $E_0 = -me^4/(2\hbar^2)$ , while Bohr radius  $a_B = \hbar^2/(me^2)$  controls the spatial extension of ground state wave function  $\psi_0(y)$ . Previous calculation shows that van der Waals interactions between the two atoms arise from the quantum fluctuations of their dipoles (the average dipole  $\langle \psi_0 | e\mathbf{y} | \psi_0 \rangle$  in the ground state vanishes).

Now we describe our main result derived in the framework of the many-body problem. We consider the so-called Saha regime, which is defined by a scaling limit, where temperature  $T$  goes to zero while density  $\rho = \rho_p = \rho_e$  vanishes exponentially fast with respect to  $T$  (see Sec. II). In that limit, it has been proven in Refs. 15 and 16 that the system behaves as a mixture of ideal gases of protons, electrons, and hydrogen atoms with densities  $\rho_p^{\text{id}} = \rho_e^{\text{id}} = \rho_f^{\text{id}}$  and  $\rho_{\text{at}}^{\text{id}}$ , which are determined as functions of  $\rho$  and  $T$  by a simple mass action law (this gives a precise meaning to the atomic recombination of a proton-electron pair in a quantum plasma). Effective potentials are exactly computed from large-distance equilibrium correlations between protons and electrons, at sufficiently low but finite temperature and density. Let  $\rho_{pp}^{(2)T}(r)$  be the proton-proton correlation (i.e., the truncated proton-proton distribution function) at given temperature  $T$  and density  $\rho$ . In agreement with a general result derived in any fluid phase,<sup>17,18</sup> we find that  $\rho_{pp}^{(2)T}(r)$  behaves asymptotically at large distance as

$$\rho_{pp}^{(2)T}(r) \underset{r \rightarrow \infty}{\sim} \frac{A_{pp}(T, \rho)}{r^6}. \quad (1.4)$$

Moreover, at leading order in the Saha regime, amplitude  $A_{pp}(T, \rho)$  takes the form of a sum of three contributions ( $\beta = 1/(k_B T)$ ),

$$A_{pp}(T, \rho) = -\beta \{ [\rho_f^{\text{id}}]^2 C^{\text{f-f}}(T) + 2\rho_f^{\text{id}} \rho_{\text{at}}^{\text{id}} C^{\text{f-at}}(T) + [\rho_{\text{at}}^{\text{id}}]^2 C^{\text{at-at}}(T) \} (1 + \mathcal{O}(e^{-\delta/k_B T})), \quad (1.5)$$

with  $\delta > 0$ . The corresponding behaviors, for the electron-proton or electron-electron correlations, are identical to Eqs. (1.4) and (1.5). In Eq. (1.5), leading terms are quadratic in the ideal free and atomic densities, in agreement with the fact that, in the Saha regime, a proton can be thought of as either being free or belonging to a hydrogen atom. This allows us to introduce three potentials  $U^{\text{f-f}}(r) = C^{\text{f-f}}/r^6$ ,  $U^{\text{f-at}}(r) = C^{\text{f-at}}/r^6$ , and  $U^{\text{at-at}}(r) = C^{\text{at-at}}/r^6$ , which describe effective interactions at large distances between either two free charges, a free charge and an atom, or two atoms, respectively. Exponentially small terms  $\mathcal{O}(\exp(-\delta/k_B T))$ ,  $\delta > 0$  include higher-order density effects, like those associated with the formation of molecules or ions for instance, as well as contributions from excited or ionized atomic states.

*Effective atom-atom interactions.* The effective atom-atom potential  $U^{\text{at-at}}(r)$  does exhibit the  $1/r^6$ -tail characteristic of van der Waals interactions. That behavior is valid for  $r$  larger than Debye screening length  $\kappa_D^{-1} = (8\pi\beta e^2 \rho_f^{\text{id}})^{-1/2}$ , which is associated with the almost classical and weakly coupled plasma of free protons and free electrons [de Broglie thermal wavelengths  $\lambda_{p,e} = (\beta\hbar^2/m_{p,e})^{1/2}$  and Bjerrum length  $\beta e^2$  are small compared to the mean interparticle distance]. Thus, and as expected, free charges do not perfectly screen van der Waals interactions. The temperature-dependent strength  $C^{\text{at-at}}(T)$  of  $U^{\text{at-at}}(r)$  reads

$$C^{\text{at-at}}(T) = - \sum_{p_a \neq 0, p_b \neq 0} \frac{|\langle \psi_0^{(a)} \otimes \psi_0^{(b)} | D^{\text{at-at}} | \psi_{p_a}^{(a)} \otimes \psi_{p_b}^{(b)} \rangle|^2}{E_{p_a} + E_{p_b} - 2E_0} \times \left[ \frac{1}{E_{p_a} + E_{p_b} - 2E_0} - \frac{2k_B T}{(E_{p_a} - E_0)(E_{p_b} - E_0)} \right]. \quad (1.6)$$

When  $T$  goes to zero,  $C^{\text{at-at}}(T)$  reduces to  $C_{\text{vdW}}$ , so  $U^{\text{at-at}}(r)$  becomes identical to  $U_{\text{vdW}}(r)$  at distances  $r$  larger than Debye length  $\kappa_D^{-1}$ . Thus, in the zero-temperature limit, free charges do not screen at all van der Waals interactions, in agreement with heuristic findings described in Sec. I A.

Partial screening of van der Waals interactions by free charges occur at finite (nonzero) temperature. The corresponding contribution to strength  $C^{\text{at-at}}(T)$  is linear in  $T$ , and does not depend on the density of free charges, since it does not depend on ionization rate  $\rho_f^{\text{id}}/\rho$  which can take arbitrary values [for  $a_B \ll r \ll \kappa_D^{-1}$ ,  $U^{\text{at-at}}(r)$  does reduce to  $U_{\text{vdW}}(r)$ , so the linear term in  $T$  in Eq. (1.6) does account for free-charge screening at  $r \gg \kappa_D^{-1}$ ]. Contribution of free charges does not depend too on their masses, contrarily to what would be expected according to naive arguments about their inertia. The negative sign of the corresponding correction in Eq. (1.6) implies that  $|C^{\text{at-at}}(T)| < |C_{\text{vdW}}|$ , so partial screening

leads to a weakening of van der Waals interactions, as both expected and observed. Notice that a derivation of Eq. (1.6) in a simpler model consisting of two atoms immersed in a classical plasma can be found in Ref. 19.

*Effective charge-atom interactions.* The effective potential  $U^{f\text{-at}}(r)$  between a free charge and an atom also exhibits a  $1/r^6$ -tail à la van der Waals for  $r \gg \kappa^{-1}$ . Its strength  $C^{f\text{-at}}(T)$  is

$$C^{f\text{-at}}(T) = -\frac{\hbar^2}{24mk_B T} \sum_{p \neq 0} \sum_{\mu=1}^3 |\langle \psi_p | D_{\mu}^{f\text{-at}} | \psi_0 \rangle|^2 \times \left[ \frac{1}{E_p - E_0} - \frac{6k_B T}{(E_p - E_0)^2} + \frac{12(k_B T)^2}{(E_p - E_0)^3} \right], \quad (1.7)$$

with

$$D_{\mu}^{f\text{-at}} = e^2 [\hat{\mathbf{u}}_{\mu}^{(a)} \cdot \mathbf{y}^{(b)} - 3(\hat{\mathbf{u}}_{\mu}^{(a)} \cdot \hat{\mathbf{r}})(\mathbf{y}^{(b)} \cdot \hat{\mathbf{r}})], \quad (1.8)$$

where for  $\mu=1,2,3$   $\hat{\mathbf{u}}_{\mu}$  is a unit vector along the  $\mu$  axis. Here  $D_{\mu}^{f\text{-at}}$  refers to the interaction between the atomic dipole  $e\mathbf{y}$  at the mass-center position  $\mathbf{r}_b$  and a reference dipole  $e\hat{\mathbf{u}}_{\mu}$  located at  $\mathbf{r}_a$ . The potential  $U^{f\text{-at}}(r)$  results from quantum fluctuations of the dipoles carried by the atom on the one hand, and by the free charge surrounded by its polarization cloud on the other hand. Atomic dipole fluctuations are of order  $e^2 a_B^2$ , while their free-charge counterparts are of order  $e^2 \lambda_{p,e}^2$ . This explains the  $1/T$  behavior of  $C^{f\text{-at}}(T)$  when  $T$  goes to zero.

Contrarily to the case of atom-atom interactions, screening by free charges determines the leading behavior of  $C^{f\text{-at}}(T)$ . In fact, at distances  $\lambda_{p,e} \ll r \ll \kappa_D^{-1}$ ,  $U^{f\text{-at}}(r)$  is identical to the  $1/r^4$  potential computed in the vacuum for an atom and a single charge, i.e.,

$$U^{f\text{-at}}(r) \sim \frac{C_0}{r^4}, \quad (1.9)$$

with negative constant

$$C_0 = - \sum_{p \neq 0} \frac{|\langle \psi_p | e^2 \mathbf{y} \cdot \hat{\mathbf{r}} | \psi_0 \rangle|^2}{E_p - E_0}. \quad (1.10)$$

Similarly to the calculation of  $C_{\text{vdW}}$ , expression (1.10) for  $C_0$  is derived from a perturbative treatment of the dipole-charge  $1/r^2$  potential up to second order. When  $r$  is increased and becomes of order the screening length  $\kappa_D^{-1}$ ,  $U^{f\text{-at}}(r)$  takes a Debye screened form proportional to  $e^{-2\kappa_D r}/r^4$ . Beyond that crossover regime, for  $r \gg \kappa_D^{-1}$ ,  $U^{f\text{-at}}(r)$  decays as  $r^{-6}$  and is no longer of the charge-dipole type.

Beyond its main effect, which is to screen the monopole carried by a single charge, the surrounding plasma also partially screens the atomic dipole at finite temperature. This gives rise to the linear and quadratic terms in  $T$  in Eq. (1.7).

*Effective charge-charge interactions.* The effective potential  $U^{f\text{-f}}(r)$  between two free charges also decays as  $1/r^6$ . It takes the form already derived in a fully ionized plasma phase,<sup>20</sup> with its strength  $C^{f\text{-f}}(T)$  given by

$$C^{f\text{-f}}(T) = -\frac{\hbar^4 e^4}{960m^2(k_B T)^3}. \quad (1.11)$$

Like for usual van der Waals forces, the  $1/r^6$  tail in  $U^{f\text{-f}}(r)$  arises because fluctuating dipoles associated with quantum charges and their screening clouds cannot be perfectly screened. Notice that potential  $U^{f\text{-f}}(r)$  is always attractive irrespective of the charge signs, and it depends on the symmetrized combination  $m=m_p m_e/(m_p+m_e)$  of proton and electron masses.

Similarly to the case of  $U^{f\text{-at}}(r)$ , the behavior of  $U^{f\text{-f}}(r)$  drastically changes when  $r$  crosses  $\kappa_D^{-1}$ . For  $\lambda_{p,e} \ll r \ll \kappa_D^{-1}$ ,  $U^{f\text{-f}}(r)$  reduces to the bare  $1/r$ -Coulomb potential of course. For  $r \sim \kappa_D^{-1}$ ,  $U^{f\text{-f}}(r)$  behaves as the exponentially screened Debye potential, while the  $1/r^6$  tail appears for  $r \gg \kappa_D^{-1}$ .

## C. Organization of the paper

In Sec. II, we recall how the Saha regime can be properly defined within a scaling limit introduced in the grand-canonical ensemble. We provide the asymptotic expressions of the corresponding ideal densities of free charges and hydrogen atoms. The hierarchy of relevant length scales is also presented.

Section III is devoted to the description of the formalism based on the path integral representation of the quantum Coulomb gas. In that representation (Sec. III A), the system can be viewed as a classical gas of random charged loops (see Ref. 17 and the review<sup>11</sup> for more references about the applications of this formalism). Coulomb divergences in familiar Mayer series for the gas of loops are removed via chain resummations (Sec. III B). This provides an effective screened potential, the quantum analog of the classical Debye potential, extensively studied in Ref. 21. We display the basic mechanism that leads to asymptotic dipolar interactions between loops, which is the root of algebraic correlations between quantum charges. A further reorganization of the Mayer series, the screened cluster expansion,<sup>22</sup> provides (nondivergent) Mayer graphs in direct correspondence with the bound entities (atoms and molecules) that can possibly occur, as well as the Mayer bonds representing their mutual interactions (Sec. III C). Eventually, we derive the leading low-temperature weights of loop clusters associated with single charges or hydrogen atoms, as well as the large-distance asymptotics of their mutual interactions (Sec. III D).

In Sec. IV, we first describe the general result about the  $1/r^6$  decay of particle correlations. The screened cluster expansion<sup>22</sup> of such correlations is used for first determining the structure of all the  $1/r^6$ -decaying graphs. Then, we show that only a few graphs contribute to the amplitude of  $1/r$  tails at leading order in the Saha regime. According to an analysis similar to that introduced for the equation of state,<sup>23</sup> we argue that the neglected graphs provide an exponentially small correction in Eq. (1.5). They include higher-order density effects, arising in part from the formation of more complex objects such as hydrogen molecules for instance.

The proper calculation of the leading behavior of amplitude  $A_{\alpha_a \alpha_b}(T, \rho)$  is presented in Sec. V. It reduces to a quadratic form in the ideal densities of free charges and hydro-

gen atoms, with temperature-dependent coefficients which are simple polynomials in  $\beta$  [see formulas (1.11), (1.7), and (1.6)]. Earlier accounts for the present results can be found in Refs. 10 and 24.

## II. THE SAHA REGIME

The Saha regime is nicely captured in a scaling limit which gives a precise meaning to the recombination of a proton-electron pair into a hydrogen atom. It is clear that the gas has to be sufficiently dilute, i.e.,  $a \gg a_B$  where  $a$  is the mean interparticle distance  $a = (3/(4\pi\rho))^{1/3}$ , to maintain the identity of individual atoms. The temperature has also to be sufficiently low to prevent atoms from dissociation,  $k_B T \ll |E_0|$ . The scaling limit is obtained, in the grand-canonical formalism, when one drives the temperature to zero and at the same time let the average chemical potential  $\mu = (\mu_p + \mu_e)/2$  of protons and electrons approach the value  $E_0$ . More precisely, if one introduces the temperature-dependent chemical potential<sup>25</sup>

$$\mu = \mu(\beta) = E_0 + k_B T \ln w, \quad (2.1)$$

with  $w$  a fixed parameter  $0 < w < \infty$ , then, as  $\beta \rightarrow \infty$ , the system behaves as an ideal mixture of ionized protons, ionized electrons, and hydrogen atoms in their ground state, i.e., its pressure  $P$  behaves as

$$\beta P = (\rho_p^{\text{id}} + \rho_e^{\text{id}} + \rho_{\text{at}}^{\text{id}})(1 + \mathcal{O}(e^{-c\beta})), \quad \beta \rightarrow \infty, \quad (2.2)$$

with  $c > 0$  and ideal densities

$$\rho_e^{\text{id}} = \rho_p^{\text{id}} = \rho_f^{\text{id}} = \frac{2}{(2\pi\lambda_e\lambda_p)^{3/2}} e^{\beta\mu} = \frac{2w}{(2\pi\lambda_e\lambda_p)^{3/2}} e^{\beta E_0} \quad (2.3)$$

and

$$\rho_{\text{at}}^{\text{id}} = \frac{4}{(2\pi\lambda_{\text{at}}^2)^{3/2}} e^{-\beta(E_0 - 2\mu)} = \frac{4w^2}{(2\pi\lambda_{\text{at}}^2)^{3/2}} e^{\beta E_0}, \quad (2.4)$$

where  $\lambda_{\text{at}} = (\beta\hbar^2/M)^{1/2}$  is the thermal de Broglie wavelength for the atom mass center with mass  $M = m_p + m_e$  (that result has been first proved in Ref. 15 and rederived in Ref. 16, while various derivations are reviewed in Chapter VII of Ref. 11). Discarding exponentially smaller contributions, total density  $\rho$  reduces to  $\rho_f^{\text{id}} + \rho_{\text{at}}^{\text{id}}$ . Notice that all previous densities vanish exponentially fast as  $e^{\beta E_0}$ , while the ionization rate

$$\frac{\rho_f^{\text{id}}}{\rho} = \frac{1}{1 + 2(M/m)^{3/4}w} \quad (2.5)$$

remains fixed and entirely determined by parameter  $w$ . For a given density  $\rho$  and a given temperature  $T$ , both  $\rho_f^{\text{id}}$  and  $\rho_{\text{at}}^{\text{id}}$  can be computed in terms of  $\rho$  and  $T$  at leading order, by using expressions (2.3) and (2.4) in  $\rho = \rho_f^{\text{id}} + \rho_{\text{at}}^{\text{id}}$  which provides a simple second order equation for  $w$  as a function of  $\rho$  and  $T$ .<sup>23</sup>

Asymptotic behavior (2.2) can be viewed as a rigorous derivation of the Saha equation of state, introduced long ago in the framework of the chemical picture. In that approach, the system is assumed to be an ideal mixture of three independent species: free protons, free electrons, and performed hydrogen atoms. The chemical potentials for protons and

electrons are chosen as  $\mu_p = \mu - (3k_B T/4)\ln(m_p/m_e)$  and  $\mu_e = \mu + (3k_B T/4)\ln(m_p/m_e)$ , so the corresponding ideal densities do satisfy the neutrality constraint. The chemical potential  $\mu_{\text{at}}$  for atoms has to be such that  $\mu_{\text{at}} = \mu_p + \mu_e$  by virtue of the mass action law applied to the chemical equilibrium  $p + e \rightleftharpoons H$ . The ideal densities of free charges and atoms computed within that scheme do reduce to Eqs. (2.3) and (2.4).

Above rigorous results can be interpreted within simple physical arguments. Choice (2.1) for the chemical potential controls the proper energy-entropy balance which favors the presence of free charges and hydrogen atoms: their occurrence probabilities exponentially dominate that of all other possible complex entities made with  $N_p$  protons and  $N_e$  electrons. This is a consequence of the existence<sup>26</sup> of some positive constant  $B$  strictly less than  $|E_0|$ , such that

$$E_{N_p, N_e} \geq -B(N_e + N_p - 1), \quad (N_e, N_p) \neq (0, 0), (1, 1), \quad (2.6)$$

where  $E_{N_p, N_e}$  is the infimum of the spectrum of  $H_{N_p, N_e}$ . In particular, hydrogen molecules are very scarce since their ideal density, of order  $\exp[-\beta(E_{2,2} - 4\mu)]$ , is indeed exponentially smaller than  $\rho_{f,\text{at}}^{\text{id}}$  by virtue of the known inequality  $E_{2,2} > 3E_0$  [consistent with the specific form of Eq. (2.6) for  $N_p = 2$  and  $N_e = 2$ ]. Scaling form (2.1) of  $\mu$  also enforces quite diluted conditions, with an exponentially vanishing density  $\rho$  of order  $\exp(\beta E_0)$ . The following hierarchy between the various relevant length scales then emerges

$$a_D \ll \lambda_{p,e,\text{at}} \ll \beta e^2 \ll a \ll \kappa_D^{-1}, \quad (2.7)$$

since  $\lambda_{p,e,\text{at}}$  is of order  $\beta^{1/2}$ , while  $a$  and  $\kappa_D^{-1}$  behaves as  $\exp(-\beta E_0/3)$  and  $\exp(-\beta E_0/2)$ , respectively. Degeneracy effects for free charges and hydrogen atoms are weak because  $\lambda_{p,e,\text{at}} \ll a$ . Moreover, charge-charge, charge-atom, and atom-atom interactions, with respective orders  $e^2/a$ ,  $e^2 a_B/a^2$ , and  $e^2 a_B^2/a^3$ , are small compared to  $k_B T$ . According to those arguments, the system indeed reduces, in the scaling limit, to an ideal mixture of free charges and hydrogen atoms.

Rigorous results for particle correlations in the Saha regime are not available. In fact, the mathematical methods involved in above proofs are well suited for studying only thermodynamics. In Secs. IV and V we determine the (exact) leading behavior of correlations by using their screened cluster expansions.<sup>22</sup> That formalism has been applied to the derivation of low-temperature expansions for thermodynamical quantities beyond Saha theory.<sup>23</sup> It provides the first corrections to the ideal Saha equation of state, at small but finite temperatures (they involve contributions of interactions between free charges and hydrogen atoms, as well as contributions from molecules  $H_2$ , ions  $H^-$ , and  $H_2^+$ , ...). Here, for particle correlations, we determine only leading terms arising from a few simple graphs, and we argue that all other contributions can be neglected.

## III. THE SCREENED CLUSTER EXPANSION

The screened cluster expansion is a generalization of the usual quantum cluster expansion suitably modified to take into account the screening effects due to the long range of

the Coulomb potential. It is worked out in Ref. 22 and we state here the definitions and the final diagrammatic rules.

## A. Loop formalism

The starting point of the analysis relies on a classical-like representation of the partition function (the so-called magic formula) obtained by using the Feynman-Kac path integral formula and collecting permutations with the same cycle structures as follows.

$$\Xi_\Lambda = \sum_{N=0}^{\infty} \frac{1}{N!} \int \prod_{i=1}^N d\mathcal{L}_i z(\mathcal{L}_i) \exp[-\beta U(\mathcal{L}_1, \dots, \mathcal{L}_N)], \quad (3.1)$$

provided that a suitable definition of the phase space integration and of the interaction are given. In various forms, this representation has been known since a long time starting with the work of Ginibre on the convergence of quantum virial expansions.<sup>27</sup> The present form (3.1) has been derived and applied by Cornu<sup>17</sup> to Coulomb systems and we follow here the definitions given in Chap. V of Ref. 11. A self-contained derivation can also be found in Ref. 28.

An element of phase space  $\mathcal{L}$ , called a loop, is a collection of  $q$  particles of the same species exchanged in a cycle. A loop

$$\mathcal{L} = (\mathbf{R}, \alpha, q, \mathbf{X}(s)), \quad 0 \leq s \leq q \quad (3.2)$$

is specified by its position  $\mathbf{R}$  in space, a particle species  $\alpha$  ( $\alpha=p, e$ ), a number of particles  $q$ , and a shape  $\mathbf{X}(s)$  with  $\mathbf{X}(0)=\mathbf{X}(q)=0$ . The closed path

$$\mathbf{R}(s) = \mathbf{R} + \lambda_\alpha \mathbf{X}(s), \quad 0 \leq s \leq q \quad (3.3)$$

links the positions of the  $q$  particles, which are located at  $\mathbf{R}(k-1)$ ,  $k=1, \dots, q$ . The path  $\mathbf{X}(s)$  is distributed according to a normalized Gaussian measure  $D(\mathbf{X})$ , with covariance

$$\int D(\mathbf{X}) X_\mu(s) X_\nu(t) = \delta_{\mu,\nu} q \left[ \min\left(\frac{s}{q}, \frac{t}{q}\right) - \frac{st}{q^2} \right], \quad \mu, \nu = 1, 2, 3. \quad (3.4)$$

Integration over phase space means integration over space and summation over all internal degrees of freedom of the loop [which we denote collectively by  $\chi=(\alpha, q, \mathbf{X})$ ] as follows:

$$\begin{aligned} \int d\mathcal{L} \cdots &= \int d\mathbf{R} \int d\chi \cdots \\ &= \int d\mathbf{R} \sum_{\alpha=p,e} \sum_{q=1}^{\infty} \int D(\mathbf{X}) \cdots . \end{aligned} \quad (3.5)$$

The interaction energy of  $N$  loops is the sum of two-body interaction potentials

$$U(\mathcal{L}_1, \dots, \mathcal{L}_N) = \sum_{1 \leq i < j}^N e_{\alpha_i} e_{\alpha_j} V(\mathcal{L}_i, \mathcal{L}_j), \quad (3.6)$$

with the interaction between two different loops

$$V(\mathcal{L}_i, \mathcal{L}_j) = \int_0^{q_i} ds \int_0^{q_j} dt \tilde{\delta}(s-t) V(\mathbf{R}_i(s) - \mathbf{R}_j(t)). \quad (3.7)$$

In Eq. (3.7),  $\tilde{\delta}(s) = \sum_{n=-\infty}^{\infty} \delta(s-n)$  is the Dirac comb of period one. Hence  $V(\mathcal{L}_i, \mathcal{L}_j)$  is the sum of the interactions between the particles in the loop  $\mathcal{L}_i$  and the particles in the loop  $\mathcal{L}_j$ . The loop potential is clearly a function of the relative distance  $\mathbf{R}_i - \mathbf{R}_j$  and of the internal constitution of the loops as follows:

$$V(\mathcal{L}_i, \mathcal{L}_j) = V(\mathbf{R}_i - \mathbf{R}_j, \chi_i, \chi_j). \quad (3.8)$$

Eventually, the activity of a loop reads

$$\begin{aligned} z(\mathcal{L}) = z(\chi) &= (-1)^{q-1} \frac{z_\alpha^q}{q (2\pi q \lambda_\alpha^2)^{3/2}} e^{-\beta U(\mathcal{L})}, \\ z_\alpha &= \exp(\beta \mu_\alpha), \end{aligned} \quad (3.9)$$

where

$$\begin{aligned} U(\mathcal{L}) &= \frac{e_\alpha^2}{2} \int_0^q ds_1 \int_0^q ds_2 (1 - \delta_{[s_1], [s_2]}) \tilde{\delta}(s_1 - s_2) \\ &\quad \times V(\mathbf{R}(s_1) - \mathbf{R}(s_2)) \end{aligned} \quad (3.10)$$

is the sum of the mutual interactions of the particles within a loop [the factor  $(1 - \delta_{[s_1], [s_2]})$ , where  $[s]$  denotes the integer part of  $s$ , excludes the self-energies of the  $q$  particles]. The above rules define the statistical mechanics of the system of charged loops, which we call the loop representation of the quantum plasma. Note that the interaction potential (3.7) inherited from the Feynman-Kac formula is not equal to the electrostatic interaction between two classical charged wires, which would be

$$V_{\text{elec}}(\mathcal{L}_i, \mathcal{L}_j) = \int_0^{q_i} ds \int_0^{q_j} dt V(\mathbf{R}_i(s) - \mathbf{R}_j(t)). \quad (3.11)$$

Although the formalism of loops has a classical structure, there is a fundamental difference between  $V(\mathcal{L}_i, \mathcal{L}_j)$  (3.7) and  $V_{\text{elec}}(\mathcal{L}_i, \mathcal{L}_j)$ , namely, the occurrence of the equal time condition  $\tilde{\delta}(s-t)$  which characterizes the quantum mechanical aspect of the interaction (3.7). This difference is responsible for the absence of exponential screening in the quantum plasma<sup>9</sup> and, as we show in the present paper, for the van der Waals forces in a partially ionized gas.

In the loop representation, we can define the loop distribution functions according to the usual definitions. Introducing the loop density  $\hat{\rho}(\mathcal{L}) = \sum_i \delta(\mathcal{L}, \mathcal{L}_i)$ , the average loop density and the loop density fluctuations for noncoincident loops are

$$\begin{aligned} \rho(\mathcal{L}) &= \langle \hat{\rho}(\mathcal{L}) \rangle, \\ \rho^{(2)T}(\mathcal{L}_1, \mathcal{L}_2) &= \langle \hat{\rho}(\mathcal{L}_1) \hat{\rho}(\mathcal{L}_2) \rangle|_{\text{n.c.}} - \langle \hat{\rho}(\mathcal{L}_1) \rangle \langle \hat{\rho}(\mathcal{L}_2) \rangle, \end{aligned} \quad (3.12)$$

where the average is taken with respect to the statistical ensemble of loops defined in Eq. (3.1), and contributions from coincident points are excluded in  $\langle \cdots \rangle|_{\text{n.c.}}$ . The truncated pair distribution of quantum particles  $\rho_{\alpha_a \alpha_b}^{(2)T}(\mathbf{r}_a, \mathbf{r}_b)$  is obtained

from  $\rho(\mathcal{L})$  and  $\rho^{(2)T}(\mathcal{L}_1, \mathcal{L}_2)$  by integration over the loop internal degrees of freedom.

$$\begin{aligned}\rho_{\alpha_a \alpha_b}^{(2)T}(\mathbf{r}_a, \mathbf{r}_b) &= \rho_{\alpha_a \alpha_b}^{(2)T\text{exch}}(\mathbf{r}_a, \mathbf{r}_b) \\ &+ \int d\chi_a \int d\chi_b q_a q_b \rho^{(2)T}(\mathcal{L}_a, \mathcal{L}_b).\end{aligned}\quad (3.13)$$

The two terms in Eq. (3.13) come from the fact that the two particles can belong either to the same loop or to two different loops. The first term on the right-hand side (two particles in the same loop) is an exchange contribution having an exponentially fast decay as  $|\mathbf{r}_a - \mathbf{r}_b| \rightarrow \infty$ .<sup>17</sup> The second term embodies the algebraic tail due to the long-range Coulomb interaction.

## B. The screened loop-loop potential

The classical-like loop formalism lends itself naturally to the introduction of Mayer graphs in the space of loops. A vertex receives the weight  $z(\mathcal{L})$  (3.9) and a bond the factor  $\exp[-\beta_{ij}V(\mathcal{L}_i, \mathcal{L}_j)] - 1$ , with  $\beta_{ij} = \beta e_{\alpha_i} e_{\alpha_j}$ . Since the loop pair potential (3.7) behaves as the Coulomb potential  $q_i e_{\alpha_i} q_j e_{\alpha_j} / |\mathbf{R}_i - \mathbf{R}_j|$  itself, the bonds are not integrable at large distances, and partial resummations are needed.

Here, we can proceed as in the standard classical case by introducing the effective screened potential  $\phi(\mathcal{L}_i, \mathcal{L}_j) = \phi(\mathbf{R}_i - \mathbf{R}_j, \chi_i, \chi_j)$  defined as the sum of chains where the bond is the linear part  $-\beta_{ij}V(\mathcal{L}_i, \mathcal{L}_j)$  of the Mayer bond. When the system is classical this leads to the well known Debye potential that decays exponentially fast with screening length  $\kappa_D^{-1}$ ,  $\kappa_D^2 = 4\pi\beta\sum_\alpha e_\alpha^2 2z_\alpha / (2\pi\lambda_\alpha^2)^{3/2}$ . The chain summation in the space of loops is worked out in Ref. 21 yielding the quantum analog of the classical Debye potential. Its Fourier transform reads

$$\begin{aligned}\tilde{\phi}(\mathbf{k}, \chi_i, \chi_j) &= \int d\mathbf{r} \exp[-i\mathbf{k} \cdot \mathbf{r}] \phi(\mathbf{r}, \chi_i, \chi_j) \\ &= \int_0^{q_i} ds_i \int_0^{q_j} ds_j \exp(i\mathbf{k} \cdot [\lambda_i \mathbf{X}_i(s_i) - \lambda_j \mathbf{X}_j(s_j)]) \\ &\times \sum_{n=-\infty}^{\infty} \frac{4\pi}{k^2 + \kappa^2(k, n)} e^{-i2\pi n(s_i - s_j)}.\end{aligned}\quad (3.14)$$

The novelty here is the occurrence of a set of screening factors for different frequencies

$$\begin{aligned}\kappa^2(k, n) &= 4\pi\beta \sum_\alpha e_\alpha^2 \sum_q \int_0^q ds \int D(\mathbf{X}) z(\chi) \\ &\times \exp(-i\mathbf{k} \cdot \lambda_\alpha \mathbf{X}(s)) \exp(i2\pi n s).\end{aligned}\quad (3.15)$$

We have to distinguish the static contribution  $n=0$  from the dynamical ones  $n \neq 0$ . By expanding the factor  $\exp(-i\mathbf{k} \cdot \lambda_\alpha \mathbf{X}(s))$  in Eq. (3.15) we see that the static term  $\kappa^2(k, n=0)$  does not vanish as  $k \rightarrow 0$  and approaches the classical Debye value  $\kappa_D^2$  at low density, whereas the dynamical terms  $n \neq 0$  vanish as

$$\kappa^2(k, n \neq 0) \sim \gamma_n k^2, \quad k \rightarrow 0. \quad (3.16)$$

More details as well as the expression of the coefficient  $\gamma_n$  can be found in Sec. III and IV of Ref. 21. It is therefore natural to decompose the potential  $\phi(\mathcal{L}, \mathcal{L}')$  between two loops  $\mathcal{L}$  and  $\mathcal{L}'$  in two parts

$$\phi = \phi^{\text{exp}} + \phi^{\text{alg}}, \quad (3.17)$$

where in  $\phi^{\text{exp}}$  we retain only the contribution of the component  $n=0$  in  $\phi$  defined in Eq. (3.14) as follows:

$$\begin{aligned}\phi^{\text{exp}}(\mathbf{k}, \chi_i, \chi_j) &= \int_0^{q_i} ds_i \int_0^{q_j} ds_j \exp(i\mathbf{k} \cdot [\lambda_i \mathbf{X}_i(s_i) \\ &- \lambda_j \mathbf{X}_j(s_j)]) \frac{4\pi}{k^2 + \kappa^2(k, n=0)}.\end{aligned}\quad (3.18)$$

Part  $\phi^{\text{exp}}(\mathbf{R}, \chi_i, \chi_j)$  decays faster than any inverse power of the relative distance  $|\mathbf{R}| = |\mathbf{R}_i - \mathbf{R}_j|$  between the two loops  $\mathcal{L}_i$  and  $\mathcal{L}_j$ , because the factor  $4\pi/(k^2 + \kappa^2(k, n=0))$  is not singular at  $k=0$ . Part  $\phi^{\text{alg}}$  is not exponentially screened because  $\kappa^2(k, n \neq 0)$  vanishes as  $k \rightarrow 0$ . In other words, the corresponding screening length diverges, so dynamical screening can only be partial in agreement with simple inertia arguments. By expanding the factor  $\exp(i\mathbf{k} \cdot [\lambda_i \mathbf{X}_i(s_i) - \lambda_j \mathbf{X}_j(s_j)])$  in  $\tilde{\phi}^{\text{alg}}(\mathbf{k}, \chi_i, \chi_j)$ , taking into account  $\int_0^q e^{2i\pi ns} ds = 0$ ,  $n \neq 0$ , and Eq. (3.16), we find that at lowest order in  $\mathbf{k}$

$$\begin{aligned}\phi^{\text{alg}}(\mathbf{k}, \chi_i, \chi_j) &\sim \int_{q_i} ds_i \int_{q_j} ds_j h(s_i - s_j) \\ &\times \frac{(\lambda_i \mathbf{X}_i(s_i) \cdot \mathbf{k})(\lambda_j \mathbf{X}_j(s_j) \cdot \mathbf{k})}{k^2},\end{aligned}\quad (3.19)$$

where  $h(s) = \sum_{n \neq 0} e^{2i\pi ns} / (1 + \gamma_n)$ . By inverse Fourier transform, we conclude that  $\phi^{\text{alg}}(\mathbf{R}, \chi_i, \chi_j)$  behaves asymptotically as the dipole potential

$$\begin{aligned}\phi^{\text{alg}}(\mathbf{R}, \chi_i, \chi_j) &\underset{|\mathbf{R}| \rightarrow +\infty}{\sim} - \int_0^{q_i} ds_i \int_0^{q_j} ds_j h(s_i - s_j) \\ &\times (\lambda_i \mathbf{X}_i(s_i) \cdot \nabla)(\lambda_j \mathbf{X}_j(s_j) \cdot \nabla) \frac{1}{|\mathbf{R}|}\end{aligned}\quad (3.20)$$

generated by the instantaneous dipoles  $e_i \lambda_i \mathbf{X}_i(s_i)$  and  $e_j \lambda_j \mathbf{X}_j(s_j)$  associated with the two loops. Notice that  $\phi^{\text{exp}}$  accounts for the exponential screening of the electrostatic part  $V_{\text{elec}}$  of  $V$ . The instantaneous dipolar part  $V - V_{\text{elec}}$  resulting from the equal-time condition in Eq. (3.7) is only partially screened and is responsible for the  $R^{-3}$  decay of  $\phi^{\text{alg}}(\mathbf{R}, \chi_i, \chi_j)$ . That  $R^{-3}$  decay of  $\phi^{\text{alg}}$  is sufficient to ensure the integrability of Mayer graphs, like in a dipole gas. The low-density behavior of  $\phi$  at finite scales is also studied in Ref. 21. At short distances  $|\mathbf{r}| \ll \kappa_D^{-1}$ ,  $\phi$  reduces to the bare Coulomb potential  $V(\mathcal{L}_a, \mathcal{L}_b)$  (3.7) between loops. At distances  $|\mathbf{r}| \sim \kappa_D^{-1}$ ,  $\phi \approx q_a q_b \exp(-\kappa_D r)/r$  approaches the standard Debye potential which describes the classical collective screening effects.

In the low-density limit, exchange effects become negligible so that loops contain only one particle ( $q_i = q_j = 1$ ); in this case we denote the shape of the loop by  $\xi(s)$ ,  $0 \leq s \leq 1$ , a closed Brownian path having the covariance (3.4) with

$q=1$ . Moreover, since  $\gamma_n \rightarrow 0$  as the density tends to zero, the function  $h(s-t)$  reduces to  $\delta(s-t)-1$  in this limit. Hence, at low density, the algebraic tail (3.20) takes the form

$$\begin{aligned} \phi_{\text{as}}(\mathbf{R}, \chi_i, \chi_j) = & - \int_0^1 ds_i \int_0^1 ds_j (\delta(s_i - s_j) - 1) (\lambda_i \xi_i(s_i) \cdot \nabla) \\ & \times (\lambda_j \xi_j(s_j) \cdot \nabla) \frac{1}{|\mathbf{R}|}. \end{aligned} \quad (3.21)$$

In the sequel, this asymptotic dipolar interaction in the space of loops will be the origin of all long-range correlations occurring between quantum charges whether they are free or bound in atoms or molecules. One can say that decomposition (3.17) of the effective potential into the rapidly decaying static part  $\phi^{\text{exp}}$  and the dipolar part  $\phi^{\text{alg}}$  offers a precise analog to the statement that free charge motion cannot screen rapid oscillations sometimes invoked in relation with shielding of van der Waals forces. Here the relevant mechanism is described consistently, in the realm of pure equilibrium statistical mechanics. Although it does not involve motion in real time, underlying dynamical aspects are implicitly incorporated in the intrinsic quantum fluctuations, which are always present.

### C. Screened cluster expansion

Standard Mayer graphs in terms of activities associated with single protons and single electrons are not well suited for a direct analysis of the Saha regime, because contributions of recombined entities (atoms, molecules, ions, etc.) cannot be easily identified. It is convenient to reorganize the diagrammatic series into graphs involving clusters of protons and electrons, together with all their mutual screened interactions and proper statistics, where clusters are in one-to-one correspondence with all possible complex entities. That reorganization, called the screened cluster expansion, is worked out in detail in Ref. 22. Here, we recall only the final diagrammatic rules for the correlation functions.

The screened cluster expansion for equilibrium quantities of the quantum electron-proton plasma involves Mayer graphs  $G$  where points are particle clusters denoted by  $C(N_e, N_p)$ , containing  $N_p$  protons and  $N_e$  electrons. Clusters are linked by interaction bonds. The internal state of a cluster involves all possible partitions of the protons and electrons into sets of protonic and electronic loops. Let

$$Q_\alpha = [q_1, \dots, q_{L_\alpha}], \quad \sum_{i=1}^{L_\alpha} q_i = N_\alpha \quad (3.22)$$

be a partition of  $N_\alpha$  into  $L_\alpha$  subsets of  $q_k$  particles,  $k = 1, \dots, L_\alpha$ , with  $q_1 \geq q_2 \geq \dots \geq q_{L_\alpha}$ . Here  $L_\alpha$  runs from 1 to  $N_\alpha$ . To a partition  $(Q_p, Q_e)$  of the  $N_p$  protons and  $N_e$  electrons, we associate a cluster of loops

$$C(Q_p, Q_e) = \{\mathcal{L}_1^{(p)}, \dots, \mathcal{L}_{L_p}^{(p)}, \mathcal{L}_1^{(e)}, \dots, \mathcal{L}_{L_e}^{(e)}\}, \quad (3.23)$$

where  $\mathcal{L}_k^{(\alpha)}$  carries  $q_k^{(\alpha)}$  particles of species  $\alpha$  ( $k=1, \dots, L_\alpha$ ). The variables associated with a cluster  $C(N_p, N_e)$  of a graph  $G$  are  $Q_p, Q_e, C(Q_p, Q_e)$ . A point corresponding to a cluster  $C$

where the associated variables are not integrated over is a root point (or white point). The integration over an internal (or black) point is performed according to the measure

$$\begin{aligned} \mathcal{D}(C) = & \sum_{Q_p, Q_e} \int \prod_{k=1}^{L_p} d\mathbf{R}_k^{(p)} \prod_{k=1}^{L_e} d\mathbf{R}_k^{(e)} \\ & \times \int \prod_{k=1}^{L_p} D(\mathbf{X}_k^{(p)}) \prod_{k=1}^{L_e} D(\mathbf{X}_k^{(e)}). \end{aligned} \quad (3.24)$$

Note that the integration measure  $\mathcal{D}(C)$  for a cluster point does not involve summation on particle species [unlike the measure defined in Eq. (3.5)]. The statistical weight of a cluster reads

$$Z_\phi^T(C) = \frac{\prod_{k=1}^{L_p} z_\phi(\mathcal{L}_k^{(p)}) \prod_{k=1}^{L_e} z_\phi(\mathcal{L}_k^{(e)})}{\prod_{q=1}^{N_p} n_p(q)! \prod_{q=1}^{N_e} n_e(q)!} \mathcal{B}_{\phi, N_p + N_e}^T(C(Q_p, Q_e)), \quad (3.25)$$

where  $n_\alpha(q)$  is the number of loops containing  $q$  particles of species  $\alpha$  in the partition  $Q_\alpha$ . In Eq. (3.25),  $z_\phi(\mathcal{L})$  is a renormalized loop activity

$$z_\phi(\mathcal{L}) = z(\mathcal{L}) \exp I_R(\mathcal{L}), \quad I_R(\mathcal{L}) = \frac{\beta e_\alpha^2}{2} (V - \phi)(\mathcal{L}, \mathcal{L}), \quad (3.26)$$

and the truncated Mayer coefficient  $\mathcal{B}_{\phi, N}^T$  is defined by a suitable truncation of the usual Mayer coefficient  $\mathcal{B}_{\phi, N}$  for  $N$  loops with pair interactions  $\phi$  (see Ref. 22). That truncation ensures that  $\mathcal{B}_{\phi, N}^T$  remains integrable over the relative distances between the loops when  $\phi$  is replaced by  $V$ . The two first truncated Mayer coefficients are  $\mathcal{B}_{\phi, 1}^T = 1$  and

$$\begin{aligned} \mathcal{B}_{\phi, 2}^T = & \exp(-\beta_{ab}\phi) - 1 + \beta_{ab}\phi - \frac{(\beta_{ab})^2\phi^2}{2!} \\ & + \frac{(\beta_{ab})^2\phi^3}{3!}, \quad \beta_{ab} = \beta e_{\alpha_a} e_{\alpha_b}. \end{aligned} \quad (3.27)$$

In two cases, the weight (3.25) of a *black* cluster must be modified to avoid double counting, as specified after the following definition of the bonds between clusters.

In a graph  $G$ , two clusters  $C_i$  and  $C_j$  are connected by at most one bond  $\mathcal{F}_\phi(C_i, C_j)$  which can be either  $-\beta\Phi$ ,  $\beta^2\Phi^2/2!$ , or  $-\beta^3\Phi^3/3!$ . The potential  $\Phi(C_i, C_j)$  is the total interaction potential between the loop clusters  $C_i(Q_i^{(p)}, Q_i^{(e)})$  and  $C_j(Q_j^{(p)}, Q_j^{(e)})$  in  $C_i$  and  $C_j$ , respectively, i.e.,

$$\Phi(C_i, C_j) = \Phi(C_i, C_j) = \sum_{\mathcal{L} \in \mathcal{C}_i} \sum_{\mathcal{L}' \in \mathcal{C}_j} e_\alpha e_{\alpha'} \phi(\mathcal{L}, \mathcal{L}'). \quad (3.28)$$

In order to avoid double counting the weight (3.25) of a *black* cluster is altered in the following two cases.

- (i) If  $C$  is an intermediate cluster in a convolution  $(-\beta\Phi) \star (-\beta\Phi)$ , and its internal state is determined by a single electronic or protonic loop, then its weight is

$$Z_\phi^T(C) = z_\phi(\mathcal{L}) - z(\mathcal{L}) \quad (3.29)$$

instead of  $Z_\phi^T(C) = z_\phi(\mathcal{L})$ .

- (ii) If  $C$  is a cluster connected to the rest of the graph by a single bond  $\frac{1}{2}(\beta\Phi)^2$ , and its internal state is deter-

mined by a single electronic or protonic loop, then its weight is also given by Eq. (3.29).

The screened cluster expansion of the two-body loop density  $\rho^{(2)T}(\mathcal{L}_a, \mathcal{L}_b)$  is given by

$$\begin{aligned} \rho^{(2)T}(\mathcal{L}_a, \mathcal{L}_b) = & \sum_{G_1} {}^* \frac{1}{S_{G_1}} \int D(C_{ab}) \left( \sum_{\mathcal{L}_i, \mathcal{L}_j \in \mathcal{C}_{ab}, i \neq j} \delta(\mathcal{L}_i, \mathcal{L}_a) \delta(\mathcal{L}_j, \mathcal{L}_b) \right) Z_\phi^T(C_{ab}) \int \prod_k D(C_k) Z_\phi^T(C_k) [\prod \mathcal{F}_\phi]_{G_1} \\ & + \sum_{G_2} {}^* \frac{1}{S_{G_2}} \int D(C_a) D(C_b) \left( \sum_{\mathcal{L}_i \in \mathcal{C}_a} \delta(\mathcal{L}_i, \mathcal{L}_a) \sum_{\mathcal{L}_j \in \mathcal{C}_b} \delta(\mathcal{L}_j, \mathcal{L}_b) \right) Z_\phi^T(C_a) Z_\phi^T(C_b) \int \prod_k D(C_k) Z_\phi^T(C_k) [\prod \mathcal{F}_\phi]_{G_2}. \end{aligned} \quad (3.30)$$

The sum  $\Sigma_G^*$  runs over all unlabeled topologically different connected graphs  $G$  which are no longer integrable over the relative distances between the clusters  $\{C_i\}_{i=1,\dots,n}$  when  $\phi$  is replaced by  $V$ . A graph  $G$  is connected, if for any pair  $(C_i, C_j)$  there exists at least one connecting path from  $C_i$  to  $C_j$  made with one or more bonds  $\mathcal{F}_\phi$ . Graphs  $G_1$  have a single root cluster  $C_{ab}$  that contains both loops  $\mathcal{L}_a$  and  $\mathcal{L}_b$ , whereas graphs  $G_2$  have two root clusters  $C_a$  and  $C_b$  with  $\mathcal{L}_a$  in  $C_a$  and  $\mathcal{L}_b$  in  $C_b$ . In the contribution from graphs  $G_1$ , loops  $\mathcal{L}_a$  and  $\mathcal{L}_b$  are not allowed to coincide. The symmetry factor  $S_G$  is the number of permutations of labeled/black clusters that leave the product of bonds  $[\prod \mathcal{F}_\phi]_G$  unchanged (only clusters with identical numbers of protons and electrons are permuted). Except for the constraint about the absence of integrability when  $\phi$  is replaced by  $V$  (represented by the star in  $\Sigma_G^*$ ), the graphs  $G$  have the same topological structure as the familiar Mayer diagrams: the ordinary points are replaced by particle clusters and the usual Mayer links are now the bonds  $\mathcal{F}_\phi$ .

#### D. Clusters associated with free charges and atoms: Statistical weights and large-distance interactions

In the Saha regime discussed in Sec. II, the relevant clusters are made with either a single electron, or a single proton or a proton-electron pair. All other clusters associated with more complex entities (e.g., hydrogen molecules) provide exponentially smaller contributions to the equation of state. Thus, they can be neglected at leading order, as discussed in Sec. III G and Appendix B of Ref. 22. The corresponding methods could be extended here to the study of distribution functions. We do not repeat in detail that analysis, and we only consider leading contributions arising from above relevant clusters associated with ionized protons, ionized electrons, and hydrogen atoms. Before turning to the corresponding estimations in Secs. IV and V, we first derive various asymptotic results for the statistical weights and interactions of interest.

In order to deal simultaneously with the three entities, we introduce the notation  $\mathbf{R}_C$  for the position of the mass

center of cluster  $C$ , and  $\chi_C$  for its internal degrees of freedom. If  $C^{(f)} = \mathcal{L}^{(\alpha)}$  denotes a cluster made of a single free charge of species  $\alpha$ ,

$$\mathbf{R}_{C^{(f)}} = \mathbf{r}, \quad \chi_{C^{(f)}} = \xi^{(f)}, \quad (3.31)$$

and we define the associated fluctuating dipole

$$\mathbf{x}_{C^{(f)}}(s) = e_\alpha \lambda_\alpha \xi^{(f)}(s). \quad (3.32)$$

If  $C^{(\text{at})}$  ( $\mathcal{L}^{(p)}, \mathcal{L}^{(e)}$ ) denotes a cluster associated with an atom we set

$$\begin{aligned} \mathbf{R}_{C^{(\text{at})}} &= \frac{m_e \mathbf{r}^{(e)} + m_p \mathbf{r}^{(p)}}{m_e + m_p}, \quad \chi_{C^{(\text{at})}} = (\mathbf{y}; \xi^{(e)}, \xi^{(p)}), \\ D(\chi_{C^{(\text{at})}}) &= d\mathbf{y} D(\xi^{(e)}) D(\xi^{(p)}), \end{aligned} \quad (3.33)$$

where  $\mathbf{y} \equiv \mathbf{r}^{(p)} - \mathbf{r}^{(e)}$  is the relative position of the proton and the electron in the atom. The fluctuating atomic dipole is defined by

$$\mathbf{x}_{C^{(\text{at})}}(s) = e[\mathbf{y} + \lambda \xi(s)] \quad (3.34)$$

with the corresponding relative fluctuation

$$\lambda \xi \equiv \lambda_p \xi^{(p)} - \lambda_e \xi^{(e)}, \quad (3.35)$$

where  $\lambda = (\beta \hbar^2 / m)^{1/2}$  is the thermal de Broglie wavelength for the relative particle. We also introduce the fluctuations of the mass-center position

$$\lambda_{\text{at}} \xi^{(\text{mc})}(s) = \frac{m_e \lambda_e \xi^{(e)}(s) + m_p \lambda_p \xi^{(p)}(s)}{m_e + m_p}. \quad (3.36)$$

The canonical transformation to the variables associated with mass center and relative position,  $(\mathbf{r}^{(p)}, \xi^{(p)}, \mathbf{r}^{(e)}, \xi^{(e)}) \rightarrow (\mathbf{R}_C, \xi^{(\text{mc})}, \mathbf{y}, \xi)$ , preserves the integration measure, i.e.,

$$d\mathbf{r}^{(p)} d\mathbf{r}^{(e)} = d\mathbf{R}_C d\mathbf{y}, \quad D(\xi^{(p)}) D(\xi^{(e)}) = D(\xi^{(\text{mc})}) D(\xi). \quad (3.37)$$

If cluster  $C_i$  is not the intermediate point of a convolution  $[-\beta\Phi] * [-\beta\Phi]$ , then its weight is  $Z_\phi^T(C)$  given by Eq. (3.25). For a cluster  $C^{(f)}$  which contains only a single free charge, its weight reduces, in the Saha regime, to

$$Z_\phi^T(C^{(f)}) = z_\phi(\mathcal{L}^{(\alpha)}) = z(\mathcal{L}^{(\alpha)}) \exp I_R(\mathcal{L}^{(\alpha)}) \sim \rho_f^{\text{id}}, \\ \alpha = e, p, \quad (3.38)$$

where we have used that  $I_R = \mathcal{O}(\beta e^2 \kappa_D)$  vanishes in agreement with the hierarchy (2.7) of length scales. If the cluster is associated with an atom,  $Z_\phi^T(C^{(\text{at})})$  behaves as

$$Z_\phi^T(C^{(\text{at})}) \sim \rho_e^{\text{id}} \rho_p^{\text{id}} \mathcal{B}_{\phi,2}^T(\chi_{C^{(\text{at})}}) = \rho_{\text{at}}^{\text{id}} \frac{e^{\beta E_0}}{(2\pi\lambda^2)^{3/2}} \mathcal{B}_{\phi,2}^T(\chi_{C^{(\text{at})}}),$$

$$\begin{aligned} \mathcal{B}_{\phi,2}^T(\chi_{C^{(\text{at})}}) &= \exp[\beta e^2 \phi(\mathcal{L}^{(e)}, \mathcal{L}^{(p)})] - 1 - \beta e^2 \phi(\mathcal{L}^{(e)}, \mathcal{L}^{(p)}) \\ &\quad - \frac{(\beta e^2)^2}{2!} [\phi(\mathcal{L}^{(e)}, \mathcal{L}^{(p)})]^2 \\ &\quad - \frac{(\beta e^2)^3}{3!} [\phi(\mathcal{L}^{(e)}, \mathcal{L}^{(p)})]^3. \end{aligned} \quad (3.39)$$

This follows from diagrammatic rules (3.25)–(3.27),  $I_R = \mathcal{O}(\beta e^2 \kappa_D)$ , and relation (2.4). Notice that  $\phi(\mathcal{L}^{(e)}, \mathcal{L}^{(p)})$ , hence  $\mathcal{B}_{\phi,2}^T$  and  $Z_\phi^T(C^{(\text{at})})$ , depend only on the internal atomic variables  $\chi_{C^{(\text{at})}} = (\mathbf{y}, \boldsymbol{\xi}^e, \boldsymbol{\xi}^p)$ . In the Saha regime, defined by scaling Eq. (2.1), it is shown in Sec. III B of Ref. 23 that

$$\int D(\chi_{C^{(\text{at})}}) Z_\phi^T(C^{(\text{at})}) \sim \rho_{\text{at}}^{\text{id}}. \quad (3.40)$$

[Asymptotic behavior (3.40) could be proved by the methods described in the Appendix of the present paper.] Strictly speaking, asymptotic form (3.39) of  $Z_\phi^T(C^{(\text{at})})$  contains density contributions of higher order than  $\rho_{\text{at}}^{\text{id}}$  since it still involves the effective potential  $\phi$ . The corresponding asymptotic behavior of atomic dipole fluctuations will be studied in Sec. V B.

Now, we show that interaction  $\Phi$  [defined in Eq. (3.28)] between previous clusters can be expressed in terms of mass centers and internal degrees of freedom [see Eqs. (3.31) and (3.33)] as

$$\Phi(C_1, C_2) = \Phi(\mathbf{R}_{C_1} - \mathbf{R}_{C_2}, \chi_{C_1}, \chi_{C_2}). \quad (3.41)$$

If  $C_1$  and  $C_2$  are free charges, according to definition (3.31),  $\Phi(C_1^{(f)}, C_2^{(f)}) = \phi(\mathcal{L}_1^{(f)}, \mathcal{L}_2^{(f)}) = \phi(\mathbf{r}_1 - \mathbf{r}_2, \boldsymbol{\xi}_1, \boldsymbol{\xi}_2)$  is clearly of the form (3.41) by definition (3.14) of the screened potential  $\phi$ . If  $C_1$  is an atom with electron and proton position  $\mathbf{r}_1^{(e)}$ ,  $\mathbf{r}_1^{(p)}$ , and  $C_2$  is a free charge  $e_{\alpha_2}$  at  $\mathbf{r}_2$ , we find

$$\begin{aligned} \Phi(C_1^{(\text{at})}, C_2^{(f)}) &= e_{\alpha_2} e [\phi(\mathbf{r}_1^{(p)} - \mathbf{r}_2, \lambda_p \boldsymbol{\xi}_1^{(p)}, \lambda_{\alpha_2} \boldsymbol{\xi}_2^{(f)}) \\ &\quad - \phi(\mathbf{r}_1^{(e)} - \mathbf{r}_2, \lambda_e \boldsymbol{\xi}_1^{(e)}, \lambda_{\alpha_2} \boldsymbol{\xi}_2^{(f)})]. \end{aligned} \quad (3.42)$$

Since the Fourier transform of  $f(\mathbf{r} + \mathbf{v})$  is  $\exp(-i\mathbf{k} \cdot \mathbf{v}) \tilde{f}(\mathbf{k})$ , the property

$$\begin{aligned} \phi(\mathbf{r} + \mathbf{v}, \lambda_1 \boldsymbol{\xi}_1, \lambda_2 \boldsymbol{\xi}_2) &= \phi(\mathbf{r}, \lambda_1 \boldsymbol{\xi}_1 - \mathbf{v}, \lambda_2 \boldsymbol{\xi}_2) \\ &= \phi(\mathbf{r}, \lambda_1 \boldsymbol{\xi}_1, \lambda_2 \boldsymbol{\xi}_2 - \mathbf{v}) \end{aligned} \quad (3.43)$$

immediately follows from definition (3.14). Use of Eq. (3.43) in Eq. (3.42) with  $\mathbf{r}_1^{(p)} = \mathbf{R}_{C_1} + [m_e/(m_e + m_p)] \mathbf{y}_1$  and  $\mathbf{r}_1^{(e)} = \mathbf{R}_{C_1} - [m_p/(m_e + m_p)] \mathbf{y}_1$  leads to

$$\begin{aligned} \Phi(C_1^{(\text{at})}, C_2^{(f)}) &= e_{\alpha_2} e \left[ \phi \left( \mathbf{R}_{C_1} - \mathbf{r}_2, \lambda_p \boldsymbol{\xi}_1^{(p)} - \frac{m_e}{m_e + m_p} \mathbf{y}_1, \lambda_{\alpha_2} \boldsymbol{\xi}_2^{(f)} \right) \right. \\ &\quad \left. - \phi \left( \mathbf{R}_{C_1} - \mathbf{r}_2, \lambda_e \boldsymbol{\xi}_1^{(e)} + \frac{m_p}{m_e + m_p} \mathbf{y}_1, \lambda_{\alpha_2} \boldsymbol{\xi}_2^{(f)} \right) \right], \end{aligned} \quad (3.44)$$

which is of the form (3.41). The same reasonings apply to  $\Phi(C_1^{(f)}, C_2^{(\text{at})})$  and  $\Phi(C_1^{(\text{at})}, C_2^{(\text{at})})$ . We define  $\Phi_{\text{as}}(C_i, C_j)$  as the large-distance behavior of  $\Phi(C_i, C_j)$  when the distance between the mass centers of the two clusters goes to infinity, while the relative distances inside each cluster as well as the Brownian paths are kept fixed. When the asymptotic form  $\phi_{\text{as}}$  (3.21) of the screened potential is introduced into Eq. (3.42), as well as in the corresponding expressions for  $\Phi(C_1^{(f)}, C_2^{(\text{at})})$  and  $\Phi(C_1^{(\text{at})}, C_2^{(\text{at})})$ , a straightforward calculation leads to the following result for all cases. For clusters which are either free charges or atoms,  $\Phi_{\text{as}}(C_1, C_2)$  takes the form of a dipolar interaction between the fluctuating dipoles  $\mathbf{x}_{C^{(\text{f})}}(s)$  or  $\mathbf{x}_{C^{(\text{as})}}(s)$  of the clusters defined in Eqs. (3.32) and (3.34),

$$\begin{aligned} \Phi_{\text{as}}(C_1, C_2) &= \int_0^1 ds \int_0^1 dt [\delta(s-t) - 1] \\ &\quad \times \frac{\sum_{\mu,\nu} [\mathbf{x}_{C_1}(s)]_\mu [\mathbf{x}_{C_2}(t)]_\nu d_{\mu\nu}}{|\mathbf{R}_{C_1} - \mathbf{R}_{C_2}|^3}, \end{aligned} \quad (3.45)$$

where

$$d_{\mu\nu} \equiv \partial_\mu \partial_\nu \left( \frac{1}{r} \right) \Big|_{r=1} = \delta_{\mu\nu} - 3 \hat{r}_\mu \hat{r}_\nu, \quad \hat{\mathbf{r}} = \frac{\mathbf{r}}{|\mathbf{r}|}. \quad (3.46)$$

We notice that the large-distance behavior  $\Phi_{\text{as}}(C_1, C_2)$  depends only on the relative position  $\mathbf{R}_{C_1} - \mathbf{R}_{C_2}$  of the mass centers and on the fluctuating dipoles  $\mathbf{x}_{C_1}(s)$  and  $\mathbf{x}_{C_2}(s)$ . The fluctuation  $\boldsymbol{\xi}^{(\text{mc})}$  of the atomic mass center does not occur in  $\Phi_{\text{as}}(C_1, C_2)$ .

#### IV. LARGE-DISTANCE BEHAVIOR OF QUANTUM CORRELATIONS

##### A. Slowest decaying graphs at large distances

The correlation function  $\rho_{\alpha_a \alpha_b}^{(2)T}(\mathbf{r}_a, \mathbf{r}_b)$  between two quantum charges  $e_{\alpha_a}$  at position  $\mathbf{r}_a$  and  $e_{\alpha_b}$  at position  $\mathbf{r}_b$  behaves at large distances as<sup>17,18</sup>

$$\rho_{\alpha_a \alpha_b}^{(2)T}(\mathbf{r}_a, \mathbf{r}_b) \underset{|\mathbf{r}_a - \mathbf{r}_b| \rightarrow +\infty}{\sim} \frac{A_{\alpha_a \alpha_b}(T, \rho)}{|\mathbf{r}_a - \mathbf{r}_b|^6}. \quad (4.1)$$

That general result holds in fluid phases of quantum Coulomb systems, and the amplitudes  $A_{\alpha_a \alpha_b}(T, \rho)$  depend on both the temperature and the density. Besides technical details which are described below, the  $r^{-6}$ -decay displayed in Eq. (4.1) can be easily understood as follows. According to the loop representation on the one hand, and to the dipolar behavior of the effective potential  $\phi$  on the other hand, the correlations of interest are analogous to those of a classical gas with  $r^{-3}$  pairwise interactions. A simple outlook to the corresponding Mayer diagrams shows that the linear contribu-

butions of interactions to the asymptotics of particle correlations vanish for symmetry reasons, i.e., because of the absence of permanent dipoles. The next quadratic terms in the expansion of Mayer bonds do provide  $r^{-6}$  tails. That rough argument can be recast in a precise form, by starting from the screened cluster expansion of particle correlations. First, we determine the structure of the slowest decaying graphs which contribute to  $A_{\alpha_a \alpha_b}$ .

The cluster expansion (3.30) of the two-body function  $\rho^{(2)T}(\mathcal{L}_a, \mathcal{L}_b)$  has two contributions. The first one arises from graphs  $G_1$  where the two root loops  $\mathcal{L}_a$  and  $\mathcal{L}_b$  are in the same cluster with weight  $Z_\phi^T(C_{ab})$ . Because of truncation, the Mayer coefficients  $B_{\phi,N}^T$  occurring in Eq. (3.25) have a fast decay when the distance between two loops inside the cluster becomes large. For instance,  $B_{\phi,2}^T$  falls off as the fourth power of  $\phi(\mathcal{L}_a, \mathcal{L}_b)$ , and the corresponding weight  $Z_\phi^T(C_{ab})$  decays as the inverse 12th power of the distance.

Hence the large-distance behavior of  $\rho^{(2)T}(\mathcal{L}_a, \mathcal{L}_b)$  is provided by graphs  $G_2$  where the root loops belong to different clusters. The clusters are linked by bonds  $\mathcal{F}_\phi(C, C')$  proportional either to  $\Phi(C, C')$ ,  $\Phi(C, C')^2$ , or  $\Phi(C, C')^3$ , where  $\Phi(C, C')$  is the sum of screened interactions  $\phi(\mathcal{L}_i, \mathcal{L}_j)$  between loops  $\mathcal{L}_i$  and  $\mathcal{L}_j$  which belong to  $C$  and  $C'$ , respectively. The  $A_{\alpha_a \alpha_b}/|\mathbf{r}_a - \mathbf{r}_b|^6$  tail of  $\rho_{\alpha_a \alpha_b}^{(2)T}(\mathbf{r}_a, \mathbf{r}_b)$  at large relative distances can arise either from one bond  $(1/2)[\beta\Phi(C_1, C_2)]^2$  or from the product of two bonds  $-\beta\Phi(C_1, C_2)$  and  $-\beta\Phi(C_3, C_4)$ .<sup>29</sup> The corresponding graphs belong to the two following classes. In the first class, graphs can be decomposed into two subgraphs  $G_a$  and  $G_b$  which contain  $C_a$  and  $C_b$ , respectively, and which are linked to each other only by a bond  $(1/2)[\beta\Phi(C_1, C_2)]^2$  where  $C_1$  belongs to  $G_a$  and  $C_2$  belongs to  $G_b$ . The corresponding product of bonds reads

$$\left[ \prod \mathcal{F}_\phi \right]_G = \left[ \prod \mathcal{F}_\phi \right]_{G_a} \frac{1}{2} [\beta\Phi(C_1, C_2)]^2 \left[ \prod \mathcal{F}_\phi \right]_{G_b}. \quad (4.2)$$

In each graph of the second class, two bonds  $\mathcal{F}_\phi(C_1, C_2)$  and  $\mathcal{F}_\phi(C_3, C_4)$  link two subgraphs  $G_a$  and  $G_b$ , where  $G_a$  contains  $C_a$ ,  $C_1$ , and  $C_3$ , while  $G_b$  involves  $C_b$ ,  $C_2$ , and  $C_4$  (with  $(C_1, C_2) \neq (C_3, C_4)$ ), i.e.,

$$\left[ \prod \mathcal{F}_\phi \right]_G = \left[ \prod \mathcal{F}_\phi \right]_{G_a} \beta^2 \Phi(C_1, C_2) \Phi(C_3, C_4) \left[ \prod \mathcal{F}_\phi \right]_{G_b}. \quad (4.3)$$

## B. Leading graphs in the Saha regime

As argued in Sec. III D, only graphs made with clusters  $C^{(f)}$  and  $C^{(at)}$  contribute to  $A_{\alpha_a \alpha_b}$  at leading order. Moreover, since the density is exponentially small in the Saha regime, their number of internal clusters cannot be too large (roughly speaking, the order in density to which a graph contributes to  $A_{\alpha_a \alpha_b}$ , increases with the number of its internal clusters). The corresponding maximal numbers depend on the topology of the considered graphs. For instance, graphs with structure (4.3) do not contribute at leading order, because they involve at least three clusters. For structure (4.2), if the simplest graphs with two internal clusters  $C_1 = C_a = C^{(f,at)}$  and  $C_2 = C_b$

$= C^{(f,at)}$  obviously contribute at leading order, we have also to take care about graphs where bond  $(1/2)[\beta\Phi(C_1, C_2)]^2$  appears in a convolution, as detailed further.

The analysis of the leading contributions of graphs with structure (4.2) is based on the following results. First, if  $g(\mathbf{r})$  is integrable and decays faster than  $f(\mathbf{r})$  when  $|\mathbf{r}|$  goes to infinity, the large-distance behavior of their convolution reads

$$\int d\mathbf{r}_1 f(\mathbf{r}_a - \mathbf{r}_1) g(\mathbf{r}_1 - \mathbf{r}_b) \underset{|\mathbf{r}_a - \mathbf{r}_b| \rightarrow +\infty}{\sim} f_{as}(\mathbf{r}_a - \mathbf{r}_b) g(\mathbf{k} = \mathbf{0}). \quad (4.4)$$

Second, it is convenient to split  $\Phi$  into the sum  $\Phi^{\text{exp}} + \Phi^{\text{alg}}$ , which arises from the decomposition  $\phi^{\text{exp}} + \phi^{\text{alg}}$  of the screened potential  $\phi(\mathcal{L}_k, \mathcal{L}_l)$  written in Eq. (3.17). That decomposition allows us to show that the leading term in  $Z_\phi^T(C^{(f)}) \beta\Phi(\mathbf{k} = \mathbf{0}, \chi_{C^{(f)}}, \chi_{C_i})$  is of order  $O(1)$  when  $C_i$  is a charged cluster. Indeed, it arises from

$$\Phi^{\text{exp}}(C^{(f)}, C_i) = e_{\alpha_f} \sum_{\mathcal{L}_l \in C_i} e_{\alpha_l} \phi^{\text{exp}}(\mathcal{L}^{(f)}, \mathcal{L}_l), \quad (4.5)$$

where  $\phi^{\text{exp}}$  is given by Eq. (3.18). In the Saha regime,  $\kappa^2(\mathbf{k} = \mathbf{0}, n=0)$  [defined in Eq. (3.15)] tends to  $\kappa_D^2$ . Then, by virtue of Eq. (3.38), we find at leading order

$$Z_\phi^T(C^{(f)}) \beta\Phi^{\text{exp}}(\mathbf{k} = \mathbf{0}, \chi_{C^{(f)}}, \chi_{C_i}) \sim \frac{4\pi\beta e_{C_i} e_{\alpha_f} \rho_f^{\text{id}}}{\kappa_D^2} = \frac{e C_i e_{\alpha_f}}{2e^2}, \quad (4.6)$$

where  $e_{C_i}$  is the total charge of  $C_i$ .

According to Eqs. (4.4) and (4.6), if  $C_1$  is a free charge, the coefficient of the  $1/|\mathbf{R}_{C^{(f)}} - \mathbf{R}_{C_2}|^6$  tail in the convolution  $\int D(C_1) [-\beta\Phi(C^{(f)}, C_1)] (1/2)[\beta\Phi(C_1, C_2)]^2$  is of the same order as the coefficient of the  $1/|\mathbf{R}_{C^{(f)}} - \mathbf{R}_{C_2}|^6$  tail in the single bond  $(1/2)[\beta\Phi(C^{(f)}, C_2)]^2$ . On the contrary, if  $C_1$  is an atom, previous convolution provides higher-order contributions to the  $1/R^6$  tails because of atom neutrality ( $e_{C^{(at)}} = 0$ ). Notice that contributions from graphs where a free charge cluster  $C^{(f)}$  is only linked to a charged root cluster by a bond  $-\beta\Phi$  cancel out at leading order by virtue of charge neutrality  $e\rho_p^{\text{id}} - e\rho_e^{\text{id}} = 0$  [the contribution from the latter bond introduces a multiplicative factor of form (4.6) with opposite signs for electron and proton clusters  $C^{(f)}$ ].

Eventually, leading contributions to  $A_{\alpha_a \alpha_b}$ , quadratic in the ideal densities, can be rewritten as the sum

$$A_{\alpha_a \alpha_b}^{f-f} + A_{\alpha_a \alpha_b}^{f-at} + A_{\alpha_a \alpha_b}^{at-f} + A_{\alpha_a \alpha_b}^{at-at} \quad (4.7)$$

discarding exponentially smaller terms. The contribution  $A_{\alpha_a \alpha_b}^{f-f}$  from two free charges arises from graphs shown in Fig. 1 where  $C_a$  and  $C_b$  are either an electron or a proton. The contributions  $A_{\alpha_a \alpha_b}^{f-at}$  ( $A_{\alpha_a \alpha_b}^{at-f}$ ) from a free charge and an atom comes from graphs drawn in Fig. 2 where  $C_a$  ( $C_b$ ) is a free charge and  $C_b$  ( $C_a$ ) is a hydrogen atom. The contribution  $A_{\alpha_a \alpha_b}^{at-at}$  from two atoms originates from the sole graph (Fig. 3) where both  $C_a$  and  $C_b$  are hydrogen atoms. The explicit asymptotic form at low temperatures of previous amplitudes is determined in next Sec. V.

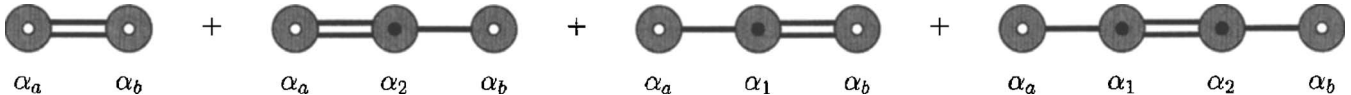


FIG. 1. Graphs which contribute to  $A_{\alpha_a \alpha_b}^{f,f}$ . A white point denotes a charge at a fixed position  $\mathbf{r}_a$  or  $\mathbf{r}_b$ , whereas a black point stands for a charge, the position of which is integrated over. A gray disk is a cluster. A solid line which links two clusters is equal to the bond  $-\beta\Phi$ . A double solid line is equal to  $\beta^2\Phi^2/2$ .

## V. AMPLITUDES OF ALGEBRAIC TAILS IN THE SAHA REGIME

### A. General structure of the various amplitudes

At leading order bonds  $-\beta\Phi$  in graphs shown in Figs. 1 and 2 can be replaced by their exponential parts  $\Phi^{\text{exp}}$ . The corresponding integrals are then easily performed by using Eq. (4.6). This provides

$$\frac{A_{\alpha_a \alpha_b}^{f,f}}{|\mathbf{r}_a - \mathbf{r}_b|^6} = \sum_{\alpha_1} \left[ \delta_{\alpha_1, \alpha_a} - \frac{4\pi\beta e_{\alpha_1} e_{\alpha_a} \rho_{\alpha_a}^{\text{id}}}{\kappa_D^2} \right] \times \sum_{\alpha_2} \left[ \delta_{\alpha_2, \alpha_b} - \frac{4\pi\beta e_{\alpha_2} e_{\alpha_b} \rho_{\alpha_b}^{\text{id}}}{\kappa_D^2} \right] W_{\alpha_1 \alpha_2}^{f,f}(|\mathbf{r}_a - \mathbf{r}_b|), \quad (5.1)$$

$$\frac{A_{\alpha_a \alpha_b}^{\text{at-at}}}{|\mathbf{r}_a - \mathbf{r}_b|^6} = \sum_{\alpha_1} \left[ \delta_{\alpha_1, \alpha_a} - \frac{4\pi\beta e_{\alpha_1} e_{\alpha_a} \rho_{\alpha_b}^{\text{id}}}{\kappa_D^2} \right] W_{\alpha_1 \alpha_b}^{\text{at-at}}(|\mathbf{r}_a - \mathbf{r}_b|), \quad (5.2)$$

and

$$\frac{A_{\alpha_a \alpha_b}^{\text{at-at}}}{|\mathbf{r}_a - \mathbf{r}_b|^6} = W_{\alpha_a \alpha_b}^{\text{at-at}}(|\mathbf{r}_a - \mathbf{r}_b|). \quad (5.3)$$

The various  $W^{i,j}$ ,  $\{i,j\}=\{f,\text{at}\}$  refer to the asymptotic interactions between electrons, protons, and atoms. Thanks to the diagrammatic rules exposed in Sec. III, and taking into account the discussion of Sec. IV, we find

$$\begin{aligned} W_{\alpha_1 \alpha_2}^{i,j}(|\mathbf{r}_a - \mathbf{r}_b|) &= \frac{\beta^2}{2} \int D(C^{(i)}) Z_\phi^T(C^{(i)}) \delta(\mathbf{r}_{\alpha_1}^{(i)} - \mathbf{r}_a) \\ &\times \int D(C^{(j)}) Z_\phi^T(C^{(j)}) \delta(\mathbf{r}_{\alpha_2}^{(j)} - \mathbf{r}_b) \\ &\times [\Phi_{\text{as}}(C^{(i)}, C^{(j)})]^2, \end{aligned} \quad (5.4)$$

where  $\Phi_{\text{as}}(\mathbf{R}_{C^{(i)}} - \mathbf{R}_{C^{(j)}}, \chi_{C^{(i)}}, \chi_{C^{(j)}})$  is the asymptotic part (3.45) of the total interaction (3.28) between clusters  $C^{(i)}$  and  $C^{(j)}$ . In Eq. (5.4),  $\mathbf{r}_\alpha^{(f)}$  ( $\alpha=e,p$ ) is the coordinate of the electron or of the proton when the cluster  $C^{(f)}$  consists of a single free charge of species  $\alpha$  and  $\mathbf{r}_\alpha^{(\text{at})}$  is the coordinate of the electron or of the proton belonging to an atomic cluster  $C^{(\text{at})}$ .

In order to obtain the final form of  $W_{\alpha_1 \alpha_2}^{i,j}(|\mathbf{r}_a - \mathbf{r}_b|)$ , we now proceed as follows. In Eq. (3.45), the decay  $|\mathbf{R}_{C^{(i)}} - \mathbf{R}_{C^{(j)}}|^{-6}$  of  $\Phi_{\text{as}}$  is written in terms of the mass centers,

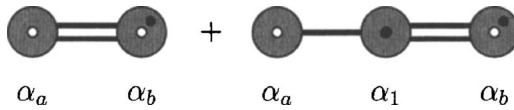


FIG. 2. Graphs which contribute to  $A_{\alpha_a \alpha_b}^{f,at}$ .

whereas the decay of the two-point correlation (4.1) is expressed in terms of the individual charge coordinates. For an atom,  $\mathbf{R}_{C^{(\text{at})}}$  differs from the electron or proton position by a quantity proportional to the relative coordinate  $\mathbf{y}$ . Hence, when charges are located at  $\mathbf{r}_a$  and  $\mathbf{r}_b$  and  $\mathbf{y}$  is kept fixed, we have

$$\frac{1}{|\mathbf{R}_{C^{(i)}} - \mathbf{R}_{C^{(j)}}|^6} = \frac{1}{|\mathbf{r}_a - \mathbf{r}_b|^6} + \mathcal{O}\left(\frac{|\mathbf{y}|}{|\mathbf{r}_a - \mathbf{r}_b|^7}\right). \quad (5.5)$$

Therefore, for computing Eq. (5.4), we can replace mass-center positions by charge coordinates in the expression (3.45) of  $\Phi_{\text{as}}$ . Inserting into Eq. (5.4) the leading behaviors of cluster weights derived in Sec. III D, we then obtain

$$\begin{aligned} W_{\alpha_1 \alpha_2}^{i,j}(|\mathbf{r}_a - \mathbf{r}_b|) &= \rho_i^{\text{id}} \rho_j^{\text{id}} \frac{\beta^2}{2} \int_0^1 ds \int_0^1 dt (\delta(s-t) - 1) \\ &\times \int_0^1 ds' \int_0^1 dt' (\delta(s'-t') - 1) \\ &\times \sum_{\mu, \nu, \rho, \sigma=1} \langle x_\mu^{(i)}(s) x_\rho^{(i)}(s') \rangle \langle x_\nu^{(j)}(t) x_\sigma^{(j)} \\ &\times (t') \rangle \frac{d_{\mu\nu} d_{\rho\sigma}}{|\mathbf{r}_a - \mathbf{r}_b|^6}, \quad |\mathbf{r}_a - \mathbf{r}_b| \rightarrow \infty, \end{aligned} \quad (5.6)$$

with  $\mathbf{x}_{C^{(i)}} = \mathbf{x}^{(i)}$ . The amplitude of the  $|\mathbf{r}_a - \mathbf{r}_b|^{-6}$  decay is determined by the square dipolar fluctuations, namely, for a single charge of type  $\alpha$

$$\begin{aligned} \langle x_\mu^{(f)}(s) x_\nu^{(f)}(s') \rangle &= (e_\alpha \lambda_\alpha)^2 \int D(\xi) \xi_\mu(s) \xi_\nu(s') \\ &= \delta_{\mu\nu} (e_\alpha \lambda_\alpha)^2 c^{(f)}(s, s'), \end{aligned} \quad (5.7)$$

with  $c^{(f)}(s, s') = (\min(s, s') - ss')$  [see Eq. (3.4)], and for an atom

$$\begin{aligned} \langle x_\mu^{(\text{at})}(s) x_\nu^{(\text{at})}(s') \rangle &= e^2 \frac{e^{\beta E_0}}{(2\pi\lambda^2)^{3/2}} \int D(\chi_{C^{(\text{at})}}) \mathcal{B}_{\phi,2}^T(\chi_{C^{(\text{at})}}) \\ &\times [y_\mu + \lambda \xi_\mu(s)][y_\nu + \lambda \xi_\nu(s')]. \end{aligned} \quad (5.8)$$

Notice that the second moments of the internal atomic variable  $\mathbf{y}$  are indeed finite thanks to the  $|\mathbf{y}|^{-12}$  decay of  $\mathcal{B}_{\phi,2}^T(\chi_{C^{(\text{at})}})$ .

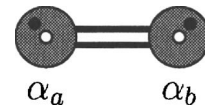


FIG. 3. Graphs which contribute to  $A_{\alpha_a \alpha_b}^{\text{at,at}}$ .

## B. Atomic dipolar fluctuation

The study of the atomic dipolar fluctuations (5.8) in the Saha regime is analogous to that presented in Sec. VI B of Ref. 30. We merely stress the similarities and differences. Since the density vanishes, the effective potential reduces to the bare Coulomb potential in the mass-center frame

$$\phi(\mathcal{L}^{(e)}, \mathcal{L}^{(p)}) \sim V(\mathbf{y}, \xi) = \int_0^1 ds \frac{1}{|\mathbf{y} + \lambda \xi(s)|} \quad (5.9)$$

at finite relative distances  $|\mathbf{y}|$ . The truncation ensures that  $\mathcal{B}_{\phi,2}^T$  remains integrable when  $\phi$  is replaced by  $V$ . However, expression (5.8) involves the second moment of  $\mathbf{y}$  which becomes nonintegrable as  $\phi$  tends to  $V$ . In order to take care of that problem, we further truncate  $\mathcal{B}_{\phi,2}^T$  by defining

$$\mathcal{B}_{\phi,2}^{TT} = e^{\beta e^2 \phi} - \sum_{n=0}^5 \frac{(\beta e^2 \phi)^n}{n!} = \mathcal{B}_{\phi,2}^T - \frac{(\beta e^2 \phi)^4}{4!} - \frac{(\beta e^2 \phi)^5}{5!} \quad (5.10)$$

so that  $\mathcal{B}_{\phi,2}^{TT}$  decays as  $|\mathbf{y}|^{-6}$ . A calculation shows that  $\mathcal{B}_{\phi,2}^{TT}$  differs from  $\mathcal{B}_{\phi,2}^T$  by a remainder  $\mathcal{R}$  which is explicitly spelled out in formulas (109), (110), and (111) of Ref. 30. We define now the dipole fluctuation by Eq. (5.8) with  $\mathcal{B}_{\phi,2}^T$  replaced by  $\mathcal{B}_{\phi,2}^{TT}$ . Its evaluation in the Saha regime requires the following.

- (i) To show that the remainder  $\mathcal{R}$  as well as the added terms to  $\mathcal{B}_{\phi,2}^T$  in Eq. (5.10) give exponentially small contributions to the atomic dipole fluctuation as  $T \rightarrow 0$ .
- (ii) To determine the low-temperature asymptotics when  $\phi$  is replaced by  $V$ .

The proof of point (i) for the remainder  $\mathcal{R}$  is the same as that presented in Appendix A 1 of Ref. 30 where the same quantity is estimated. The second moments of the added terms in Eq. (5.10) diverge at most as  $\kappa_D \sim e^{-\beta E_0/2}$  in the Saha regime [that estimation merely follows by replacing  $\phi$  by  $\exp(-\kappa_D)/y$ ]. Once multiplied by the exponentially decaying prefactor  $e^{\beta E_0}$ , they do not contribute to the leading behavior of Eq. (5.8).

Hence we come to the point (ii) by writing now  $V$  instead of  $\phi$  in Eq. (5.8) up to exponentially small terms. Using Eq. (3.37), integration on the mass-center fluctuation  $\xi^{(mc)}$  becomes straightforward because the integrand does not depend any more on  $\xi^{(mc)}$ . Thus, dipolar atomic fluctuation (5.8) reduces to

$$\begin{aligned} & e^2 \exp(\beta E_0) \int d\mathbf{y} \frac{1}{(2\hat{\pi}\lambda^2)^{3/2}} \int D(\xi) [\mathbf{y}_\mu + \lambda \xi_\mu(s)] \\ & \times [\mathbf{y}_\nu + \lambda \xi_\nu(s')] \left[ e^{\beta e^2 V(\mathbf{y}, \xi)} - \sum_{n=0}^5 \frac{(\beta e^2 V(\mathbf{y}, \xi))^n}{n!} \right] \\ & \equiv e^2 \exp(\beta E_0) K_{\mu\nu}(s-s') \end{aligned} \quad (5.11)$$

apart from exponentially decaying terms. Now, Eq. (5.11) only depends on the bare Coulomb potential. In order to determine its low-temperature asymptotics in terms of atomic eigenvalues and eigenstates, we convert  $K_{\mu\nu}(s-s')$  in

the operator formalism by applying Feynman-Kac formula backwards,

$$\begin{aligned} K_{\mu\nu}(s-s') = \text{Tr} \left\{ e^{-\beta H} T \left( q_\mu(s) q_\nu(s') - q_\mu^0(s) q_\nu^0(s') \right. \right. \\ \left. \left. \times \sum_{n=0}^5 \frac{[\beta \int_0^1 d\tau \bar{V}^0(\tau)]^n}{n!} \right) \right\}. \end{aligned} \quad (5.12)$$

The trace runs over the spectral states of the internal part  $H$  of the atom Hamiltonian,  $H=H_0+V$ ,  $H_0=|\mathbf{p}|^2/(2m)$ ,  $V=-e^2/|\mathbf{q}| \equiv -\bar{V}$ , and  $T$  is the time ordering operator;  $q_\mu(s)$  and  $q_\mu^0(s)$  are the interacting and freely (imaginary time) evolved position operators

$$\begin{aligned} q_\mu(s) &= U(-s) q_\mu U(s), \quad U(s) = e^{-sH}, \\ q_\mu^0(s) &= U_0(-s) q_\mu U_0(s), \\ \bar{V}^0(s) &= U_0(-s) \bar{V} U_0(s), \quad U_0(s) = e^{-sH_0}. \end{aligned} \quad (5.13)$$

The subtraction of the freely evolving quantities in Eq. (5.12) ensures the finiteness of the trace (that procedure implicitly accounts for screening). The leading terms at low temperature arise from the projection of  $U(s)$  on the ground state. Let  $P=|0\rangle\langle 0|$  be the corresponding projector,  $Q=I-P=\sum_{m>1}|m\rangle\langle m|$ , where the sum runs over all excited states of the hydrogen atom including the continuous spectrum. We decompose  $U(s)=U_P(s)+U_Q(s)$  accordingly, with  $U_P(s)=\exp[-E_0 s]P$  and  $U_Q(s)=U(s)Q=QU(s)$ . Then, we can split  $K_{\mu\nu}(s-s')$  into two terms

$$K_{\mu\nu}(s-s') = K_{\mu\nu}^{(1)}(s-s') + K_{\mu\nu}^{(2)}(s-s'). \quad (5.14)$$

The first term  $K_{\mu\nu}^{(1)}(s-s')$  is the part that involves at least one ground state contribution. After also writing time ordering explicitly, it reads

$$\begin{aligned} K_{\mu\nu}^{(1)}(s-s') &= \theta(s-s') \{ \text{Tr} U_P(\beta - s + s') q_\mu U_P(s-s') q_\nu \\ &+ \text{Tr} U_P(\beta - s + s') q_\mu U_Q(s-s') q_\nu \\ &+ \text{Tr} U_Q(\beta - s + s') q_\mu U_P(s-s') q_\nu \} \\ &+ \text{same expression with } (s,s') \\ &\text{and } (\mu,\nu) \text{ permuted.} \end{aligned} \quad (5.15)$$

Since  $P$  is one dimensional, traces are well defined in Eq. (5.15). The remaining part  $K_{\mu\nu}^{(2)}(s-s')$  contains the effects of excited and ionized states of both atoms together with the truncation. We show in the Appendix that it provides exponentially small contributions to atomic dipole fluctuations, namely,

$$e^2 \exp(\beta E_0) K_{\mu\nu}^{(2)}(s) = \mathcal{O}[Pol(\sqrt{\beta}) \exp(-\beta(E_1 - E_0))], \quad (5.16)$$

where  $Pol(\sqrt{\beta})$  is a polynomial in  $\sqrt{\beta}$  while  $E_1=E_0/4$  denotes the energy of the first excited states. Finally, working out the trace in the eigenstate basis of  $H$  gives the explicit form of  $K_{\mu\nu}^{(1)}(s-s')$  in terms of eigenvalues and eigenfunctions

$$K_{\mu\nu}^{(1)}(s-s') = \sum_{p,p'} c_{p,p'}^{(\text{at})}(s,s') t_{\mu\nu}(p,p') \quad (5.17)$$

with

$$\begin{aligned} c_{p,p'}^{(\text{at})}(s,s') &= e^{\beta(s-s')(E_p-E_{p'})} \{ \theta(s-s') e^{-\beta E_p} \\ &\quad + \theta(s'-s) e^{-\beta E_{p'}} \}, \end{aligned} \quad (5.18)$$

$$t_{\mu\nu}(p,p') \equiv \langle \psi_p | q_\mu | \psi_{p'} \rangle \langle \psi_{p'} | q_\nu | \psi_p \rangle = t_{\nu\mu}(p',p). \quad (5.19)$$

Since matrix element  $\langle \psi_p | q_\mu | \psi_{p'} \rangle$  is of order the Bohr radius  $a_B$ , the atomic dipole fluctuations are of order  $(ea_B)^2$  at low temperature, as expected.

### C. Low-temperature asymptotics of the various amplitudes

The low-temperature forms of the amplitudes  $A_{\alpha_a \alpha_b}^{i-j}$  are now determined by using the asymptotics of free and atomic dipole fluctuations.

*Amplitude for two free charges.* According to Eqs. (5.6) and (5.7), we find

$$W_{\alpha_1 \alpha_2}^{f-f} = [\rho_f^{\text{id}}]^2 \frac{\beta^2 e^4}{2} \lambda_{\alpha_1}^2 \lambda_{\alpha_2}^2 I^{f-f} \frac{\sum_{\mu,\nu} [d_{\mu\nu}]^2}{|\mathbf{r}_a - \mathbf{r}_b|^6} \quad (5.20)$$

with

$$\begin{aligned} I^{f-f} &\equiv \int_0^1 ds \int_0^1 dt [\delta(s-t) - 1] \int_0^1 ds' \int_0^1 dt' \\ &\quad \times [\delta(s'-t') - 1] c^{(f)}(s,s') c^{(f)}(t,t'). \end{aligned} \quad (5.21)$$

The insertion of Eq. (5.20) into Eq. (5.1) provides the amplitude  $A_{\alpha_a \alpha_b}^{f-f}$ . The corresponding summations over species  $\alpha_1$  and  $\alpha_2$  yield the same value according to

$$\sum_{\alpha_1} \left[ \delta_{\alpha_1, \alpha_a} - \frac{4\pi\beta e_{\alpha_1} e_{\alpha_a} \rho_{\alpha_a}^{\text{id}}}{\kappa_D^2} \right] \lambda_{\alpha_1}^2 = \frac{\lambda^2}{2}, \quad (5.22)$$

which follows from  $\rho_e^{\text{id}} = \rho_p^{\text{id}} = \rho_f^{\text{id}}$  and  $\kappa_D^2 = 8\pi\beta\rho_f^{\text{id}}e^2$ . Amplitude  $A_{\alpha_a \alpha_b}^{f-f}$  then reads

$$A_{\alpha_a \alpha_b}^{f-f} = -\beta [\rho_f^{\text{id}}]^2 C^{f-f} \quad (5.23)$$

with

$$C^{f-f} = -\frac{I^{f-f}}{8} \beta \lambda^4 e^4 \sum_{\mu,\nu} [d_{\mu\nu}]^2. \quad (5.24)$$

Notice that  $A_{\alpha_a \alpha_b}^{f-f}$  does not depend on considered species  $\alpha_a$  and  $\alpha_b$ . Coefficient  $C^{f-f}$  is nothing but the strength of the effective potential between two free charges as described in Sec. I B. Its explicit value (1.11) immediately follows from Eq. (5.24), where constants  $I^{f-f}$  and  $\sum_{\mu,\nu} [d_{\mu\nu}]^2$  are replaced by their numerical values  $I^{f-f} = 1/720$  and  $\sum_{\mu,\nu} [d_{\mu\nu}]^2 = 6$  computed from  $c^{(f)}(s,s') = (\min(s,s') - ss')$  and definition (3.46).

*Amplitude for a free charge and an atom.* Taking into account expression (5.7) of free dipole fluctuation, as well as the results derived in Sec. V B about atomic fluctuations (5.8), we can rewrite the corresponding expression (5.6) of  $W_{\alpha_1 \alpha_2}^{f-\text{at}}$  as

$$\begin{aligned} W_{\alpha_1 \alpha_2}^{f-\text{at}} &= \rho_f^{\text{id}} \rho_{\alpha_2}^{\text{id}} \frac{\beta^2 e^4}{2} \lambda_{\alpha_1}^2 \sum_{p,p'} e^{\beta E_0} I^{f-\text{at}}(E_p, E_{p'}) \\ &\quad \times \frac{\sum_{\mu,\nu,\sigma} d_{\mu\nu} d_{\mu\sigma} t_{\nu\sigma}(p, p')}{|\mathbf{r}_a - \mathbf{r}_b|^6}. \end{aligned} \quad (5.25)$$

Function  $I^{f-\text{at}}(E_p, E_{p'})$  is defined as  $I^{f-f}$  with  $c^{(f)}(t, t')$  replaced by its atomic counterpart  $c_{p,p'}^{(\text{at})}(t, t')$  given by expression (5.18). In writing Eq. (5.25), exponentially smaller terms arising from the contribution of  $K_{\mu\nu}^{(2)}(s-s')$  to atomic fluctuations have been omitted [see Eq. (5.16)]. Each function  $I^{f-\text{at}}(E_p, E_{p'})$  is readily evaluated as

$$\begin{aligned} I^{f-\text{at}}(E_p, E_{p'}) &= -\frac{1}{12} \frac{1}{\beta(E_p - E_{p'})} [e^{-\beta E_p} - e^{-\beta E_{p'}}] \\ &\quad - \frac{1}{2} \frac{1}{\beta^2(E_p - E_{p'})^2} [e^{-\beta E_p} + e^{-\beta E_{p'}}] \\ &\quad - \frac{1}{\beta^3(E_p - E_{p'})^3} [e^{-\beta E_p} - e^{-\beta E_{p'}}]. \end{aligned} \quad (5.26)$$

Notice that  $I^{f-\text{at}}(E_p, E_{p'}) = I^{f-\text{at}}(E_{p'}, E_p)$  and  $I^{f-\text{at}}(E_p, E_p) = 0$ . In the low-temperature limit, we find

$$\begin{aligned} e^{\beta E_0} I^{f-\text{at}}(E_p, E_0) &= \frac{1}{12\beta(E_p - E_0)} - \frac{1}{2\beta^2(E_p - E_0)^2} \\ &\quad + \frac{1}{\beta^3(E_p - E_0)^3} + \mathcal{O}(\beta^{-3} e^{-\beta(E_1 - E_0)}), \end{aligned} \quad (5.27)$$

whereas  $e^{\beta E_0} I^{f-\text{at}}(E_p, E_{p'}) = \mathcal{O}(\beta^{-3} e^{-\beta(E_1 - E_0)})$ , if  $p \neq 0$  and  $p' \neq 0$ .

Inserting Eq. (5.25) into Eq. (5.2), taking into account the asymptotics (5.27), and performing again the summation over species  $\alpha_1$  with Eq. (5.22), we obtain the low-temperature form of amplitude  $A_{\alpha_a \alpha_b}^{f-\text{at}}$ . A similar calculation applies to  $A_{\alpha_a \alpha_b}^{\text{at}-f}$  which is equal to  $A_{\alpha_a \alpha_b}^{f-\text{at}}$ , while both amplitudes are independent of particle species  $\alpha_a, \alpha_b$ . According to those considerations, the leading form of  $A_{\alpha_a \alpha_b}^{f-\text{at}}$  is rewritten as  $-\beta \rho_f^{\text{id}} \rho_{\alpha_2}^{\text{id}} C^{f-\text{at}}$  (discarding exponentially smaller corrections), where the strength  $C^{f-\text{at}} = C^{\text{at}-f}$  of the effective potential between a free charge and an atom is found to be

$$\begin{aligned} C^{f-\text{at}} &= -\frac{\hbar^2 e^4 \beta}{24m} \sum_{p \neq 0} \sum_{\mu,\nu,\sigma} d_{\mu\nu} d_{\mu\sigma} t_{\nu\sigma}(p, 0) \\ &\quad \times \left[ \frac{1}{E_p - E_0} - \frac{6}{\beta(E_p - E_0)^2} + \frac{12}{\beta^2(E_p - E_0)^3} \right], \end{aligned} \quad (5.28)$$

with  $d_{\mu\nu}$  and  $t_{\nu\sigma}(p, 0)$  defined in Eqs. (3.46) and (5.19), respectively. That formula is identical to Eq. (1.7) when expressed in terms of matrix elements of the dipolelike operator  $D_{\mu}^{f-\text{at}}$  given by Eq. (1.8).

*Amplitude for two atoms.* Similarly to the derivation of Eq. (5.25), we find (apart from exponentially smaller terms)

$$W_{\alpha_a \alpha_b}^{\text{at-at}} = [\rho_{\text{at}}^{\text{id}}]^2 \frac{\beta^2 e^4}{2} \sum_{p_1, p_2, p_3, p_4} e^{2\beta E_0} I^{\text{at-at}}(E_{p_1}, E_{p_2}, E_{p_3}, E_{p_4}) \frac{\sum_{\mu, \nu, \rho, \sigma} d_{\mu\nu} d_{\rho\sigma} t_{\mu\rho}(p_1, p_2) t_{\nu\sigma}(p_3, p_4)}{|\mathbf{r}_a - \mathbf{r}_b|^6}, \quad (5.29)$$

where  $I^{\text{at-at}}(E_{p_1}, E_{p_2}, E_{p_3}, E_{p_4})$  is defined as  $I^{f-f}$  by replacing  $c^{(f)}(t, t')$  and  $c^{(f)}(s, s')$  by  $c_{p_1, p_2}^{(\text{at})}(t, t')$  and  $c_{p_3, p_4}^{(\text{at})}(s, s')$ , respectively. Using Eq. (5.18), a straightforward calculation gives

$$\begin{aligned} I^{\text{at-at}}(E_{p_1}, E_{p_2}, E_{p_3}, E_{p_4}) &= \frac{1}{\beta(E_{p_1} + E_{p_3} - E_{p_2} - E_{p_4})} [e^{-\beta(E_{p_2} + E_{p_4})} - e^{-\beta(E_{p_1} + E_{p_3})}] \\ &\quad - \frac{1}{\beta^2(E_{p_1} - E_{p_2})(E_{p_3} - E_{p_4})} [e^{-\beta(E_{p_1} + E_{p_3})} + e^{-\beta(E_{p_2} + E_{p_4})} - e^{-\beta(E_{p_1} + E_{p_4})} - e^{-\beta(E_{p_2} - E_{p_3})}]. \end{aligned} \quad (5.30)$$

Notice that  $I^{\text{at-at}}(E_{p_1}, E_{p_2}, E_{p_3}, E_{p_4}) = I^{\text{at-at}}(E_{p_2}, E_{p_1}, E_{p_4}, E_{p_3}) = I^{\text{at-at}}(E_{p_3}, E_{p_4}, E_{p_1}, E_{p_2})$  and  $I^{\text{at-at}}(E_{p_1}, E_{p_2}, E_{p_3}, E_{p_4}) = 0$  if  $E_{p_1} = E_{p_2}$  or/and  $E_{p_3} = E_{p_4}$ . The leading terms at low temperature in  $e^{2\beta E_0} I^{\text{at-at}}(E_{p_1}, E_{p_2}, E_{p_3}, E_{p_4})$  are such that the exponential in Eq. (5.30) is equal to  $e^{-2\beta E_0}$ , namely,

$$\begin{aligned} e^{2\beta E_0} I^{\text{at-at}}(E_0, E_{p_2}, E_0, E_{p_4}) &= \frac{1}{\beta(E_{p_2} + E_{p_4} - 2E_0)} - \frac{1}{\beta^2(E_{p_2} - E_0)(E_{p_4} - E_0)} \\ &\quad + \mathcal{O}(e^{-\beta\delta}), \\ e^{2\beta E_0} I^{\text{at-at}}(E_0, E_{p_2}, E_{p_3}, E_0) &= -\frac{1}{\beta^2(E_{p_2} - E_0)(E_{p_3} - E_0)} + \mathcal{O}(e^{-\beta\delta}), \end{aligned} \quad (5.31)$$

while the other cases follow by using previous symmetry relations.

The insertion of Eq. (5.29) into Eq. (5.3) together with asymptotics (5.31) provide the low-temperature form of amplitude  $A_{\alpha_a \alpha_b}^{\text{at-at}}$ , which does not depend on species  $\alpha_a, \alpha_b$ . Then, we recast that leading amplitude as  $-\beta[\rho_{\text{at}}^{\text{id}}]^2 C^{\text{at-at}}$  (apart from exponentially smaller corrections), where strength  $C^{\text{at-at}}$  of the effective atom-atom potential reduces to

$$\begin{aligned} C^{\text{at-at}} &= -e^4 \sum_{p_1 \neq 0, p_2 \neq 0} \sum_{\mu, \nu, \rho, \sigma} d_{\mu\nu} d_{\rho\sigma} t_{\mu\rho}(p_1, 0) t_{\nu\sigma}(p_2, 0) \\ &\times \left[ \frac{1}{E_{p_1} + E_{p_2} - 2E_0} - \frac{2}{\beta(E_{p_1} - E_0)(E_{p_2} - E_0)} \right]. \end{aligned} \quad (5.32)$$

Taking into account definitions (3.46) and (5.19) of  $d_{\mu\nu}$  and  $t_{\nu\sigma}$ , respectively, we can exactly rewrite Eq. (5.32) as Eq. (1.6) with definition (1.2) of  $D^{\text{at-at}}$ .

## D. Concluding remarks

Our derivations rely on a term-by-term analysis of screened cluster expansions, where each correction to the leading contributions in the Saha regime is shown to be exponentially smaller. From a mathematical viewpoint, we have no rigorous control on the convergence of the corre-

sponding infinite sums of graphs. Nevertheless, we expect that our analysis provides the exact amplitudes of  $1/r^6$  tails in the scaling zero-temperature limit defined by parameterization (2.1) of the chemical potential. Moreover, the corresponding remainder should vanish exponentially faster than leading terms in that limit. This is the content of formula (1.5) which is the analog for particle correlations of rigorous result (2.2) for the equation of state.

Our results about  $1/r^6$  tails are valid at distances  $r$  much larger than screening length  $\kappa_D^{-1}$  which becomes exponentially large in the previous scaling limit (see Sec. II). In other words, we first define amplitude  $A_{\alpha_a \alpha_b}(T, \rho)$  by taking the limit of  $|\mathbf{r}_a - \mathbf{r}_b|^6 \rho_{\alpha_a \alpha_b}^{(2)T}(\mathbf{r}_a - \mathbf{r}_b)$  when  $|\mathbf{r}_a - \mathbf{r}_b| \rightarrow \infty$ , and afterwards we consider the low-temperature limit of  $A_{\alpha_a \alpha_b}(T, \rho)$  within scaling relation (2.1). We stress that both limits do not commute. In fact, if the scaling low-temperature limit is first taken at finite distances, the behavior of particle correlations is quite different as described below.

Now, we consider  $r = |\mathbf{r}_a - \mathbf{r}_b|$  in the range  $\beta e^2 \ll r \ll \kappa_D^{-1}$ . Collective effects can be neglected in  $\phi$  which reduces to the bare Coulomb interaction  $\int_0^1 ds |\mathbf{r}_1 - \mathbf{r}_2 + \lambda_{\alpha_1} \xi_{\alpha_1}(s) - \lambda_{\alpha_2} \xi_{\alpha_2}(s)|^{-1}$  between loops [set the screening factor for every frequency (3.15) equal to 0 in Eq. (3.14)]. Leading contributions to  $\rho_{\alpha_a \alpha_b}^{(2)T}(\mathbf{r}_a, \mathbf{r}_b)$  then arise from the simplest graphs with two root clusters and no black cluster (contributions from graphs with a single root clusters are smaller by factors which involve positive powers of  $\beta e^2/r$  and  $a_B/r$  thanks to truncation in  $\mathcal{B}_{V,N}^T$ ). Again, the various contributions can be rewritten in terms of effective interactions between either two free charges, a free charge and an atom, or two atoms.

For two free charges, the resulting effective potential  $U^{f-f}(r)$  arises from the graph with single-charge root clusters connected by a bond  $-\beta\Phi$ . It does reduce to the Coulomb potential  $e_{\alpha_a} e_{\alpha_b}/r$ , in agreement with classical condition  $\lambda_e, \lambda_p \ll r$  which follows from the hierarchy of length scales (2.7) which prevail in the Saha regime.

For a free charge and an atom,  $U^{\text{at-at}}(r)$  is given by the graph with a single-charge root cluster  $C_a^{(f)}$  connected by a bond  $\beta^2 \Phi^2/2$  to an atomic root cluster  $C_b^{(\text{at})}$ . Taking into account that the free charge remains unscreened and can be treated classically, the corresponding potential  $\Phi(C_a^{(f)}, C_b^{(\text{at})})$  can be replaced by the charge-dipole form

$$e_{\alpha_a} \int_0^1 ds \mathbf{x}_{C_b^{(\text{at})}}(s) \cdot \nabla \left( \frac{1}{r} \right), \quad (5.33)$$

since  $r \gg a_B$  in the considered range [see hierarchy (2.7)]. The rest of the calculation is analogous to that performed in Sec. V. As already noticed in Ref. 23, the corresponding leading contribution does reduce to the  $1/r^4$  potential (1.9) obtained from an elementary second-order perturbation calculation in vacuum.

For two atoms,  $U^{\text{at-at}}(r)$  comes from the graph with two atomic root clusters connected by a bond  $\beta^2 \Phi^2/2$ . Taking again into account  $r \gg a_B$ , potential  $\Phi(C_a^{(\text{at})}, C_b^{(\text{at})})$  can be replaced by

$$\frac{1}{r^3} \int_0^1 ds \sum_{\mu, \nu} [\mathbf{x}_{C_a^{(\text{at})}}(s)]_\mu [\mathbf{x}_{C_b^{(\text{at})}}(s)]_\nu d_{\mu\nu}. \quad (5.34)$$

Notice that Eq. (5.34) differs from asymptotic expression (3.45) valid at  $r \gg \kappa_D^{-1}$ , by substitution  $\delta(s-t)-1 \rightarrow \delta(s-t)$  which accounts for the absence of partial screening at  $r \ll \kappa_D^{-1}$ . A calculation similar to that performed in Sec. V then shows that  $U^{\text{at-at}}(r)$  does reduce to the van der Waals potential  $U_{\text{vdW}}(r)$  computed in the vacuum, apart from exponentially smaller terms (that behavior is also quoted in Ref. 23).

## APPENDIX: RIGOROUS BOUNDS FOR THE CONTRIBUTIONS OF EXCITED STATES TO DIPOLAR FLUCTUATIONS

Term  $K_{\mu\nu}^{(2)}(s-s')$  defined by decomposition (5.14) of expression (5.12) reads

$$K_{\mu\nu}^{(2)}(s) = \text{Tr} \left\{ \begin{aligned} & \mathcal{T}[U_Q(\beta-s)q_\mu U_Q(s)q_\nu] \\ & - \mathcal{T} \left[ U_0(\beta-s)q_\mu U_0(s)q_\nu \sum_{n=0}^5 \frac{[\beta f_0^1 d\tau \bar{V}^0(\tau)]^n}{n!} \right] \end{aligned} \right\}. \quad (A1)$$

Trace (A1) is the same as that occurring in formula (A27) of Ref. 30 with the  $B_k$  (A28) replaced by the components  $q_\mu$  of the position operator. Thus, in order to obtain the estimate (5.16), we can follow step by step the analysis of Appendix A 2 of Ref. 30 (the Lemma 3 of Ref. 30 with  $q_\mu$  in place of  $B_k$  relies on Lemma 5 in place of Lemma 8).

We now supplement Appendix A 3 of Ref. 30 by providing proofs of the basic Lemmas 4–6 which were stated there without demonstration. We set units such that  $e^2=1$  and  $\hbar^2/m=1$ , so  $V(\mathbf{x})=-1/|\mathbf{x}|$  and  $U_0(s)=\exp(-s|\mathbf{p}|^2/2)$ ,  $\|U_0(s)\|=1$ . Notation  $\|\cdot\|$  stands for the operator norm and  $C$  denotes a constant which may have different values at different places.

**Lemma 4:** The operator  $U_0(s)V$  is bounded for  $s>0$

$$\|VU_0(s)\| = \|U_0(s)V\| \leq C \left( \frac{1}{\sqrt{s}} + 2 \right). \quad (A2)$$

**Proof:** The well known inequality<sup>31</sup>  $\|V\varphi\| \leq 2\|\mathbf{p}\|\varphi\|$  implies  $\|V(|\mathbf{p}|+1)^{-1}\varphi\| \leq 2\|\mathbf{p}\|(|\mathbf{p}|+1)^{-1}\varphi\| \leq 2\|\varphi\|$  for a dense set of smooth functions  $\varphi(\mathbf{x})$  in  $L^2(\mathbb{R}^3)$ . Hence  $V(|\mathbf{p}|+1)^{-1}$  is bounded and

$$\begin{aligned} \|VU_0(s)\| &= \|V(|\mathbf{p}|+1)^{-1}(|\mathbf{p}|+1)\exp(-s|\mathbf{p}|^2/2)\| \\ &\leq 2\|(|\mathbf{p}|+1)\exp(-s|\mathbf{p}|^2/2)\|. \end{aligned} \quad (A3)$$

The result follows from the fact that the function  $y \exp(-y^2/2)$  is bounded for  $y \geq 0$ .

**Lemma 5:** The following commutators are bounded:

$$\|[q_\mu, U_0(s)]\| \leq C\sqrt{s}, \quad (A4)$$

$$\|[q_\mu, U_0(s)]V\| \leq C(1+\sqrt{s}), \quad (A5)$$

$$\|[q_\mu, [q_\nu, U_0(s)]]V\| \leq C\sqrt{s}(1+\sqrt{s}). \quad (A6)$$

**Proof:** The canonical commutation relations imply

$$[q_\mu, U_0(s)] = is p_\mu U_0(s). \quad (A7)$$

Thus

$$\|[q_\mu, U_0(s)]V\| \leq \sqrt{s} \|\sqrt{s} p_\mu U_0(s/2)\| \|U_0(s/2)V\|$$

and Eq. (A5) follows from the Lemma 1 and the boundedness of  $y \exp(-y^2/4)$ ,  $y \geq 0$ . The estimate (A6) is obtained in the same way by using

$$[q_\mu, [q_\nu, U_0(s)]] = is \delta_{\mu\nu} U_0(s) - s^2 p_\mu p_\nu U_0(s).$$

**Lemma 6:** The operator  $U_0(s)VU_0(t)V$ ,  $s, t > 0$  belongs to the Hilbert-Schmidt class for  $s, t > 0$

$$\|U_0(s)VU_0(t)V\|_2 \leq \frac{C}{\sqrt{t(s+t)}}, \quad s, t \geq 0. \quad (A8)$$

Here  $\|A\|_2 = (\int d\mathbf{x} \int d\mathbf{y} |\langle \mathbf{x}|A|\mathbf{y} \rangle|^2)^{1/2}$  is the Hilbert-Schmidt norm of  $A$ .

**Proof:** We give a few steps of the calculation. Let

$$F(\mathbf{x}, \mathbf{y}, s, t) = \langle \mathbf{x} | e^{-sH_0} \frac{1}{|\mathbf{r}|} e^{-tH_0} | \mathbf{y} \rangle, \quad s, t > 0,$$

which, after introducing the explicit form of free kernel  $\langle \mathbf{x} | e^{-sH_0} | \mathbf{y} \rangle = (2\pi s)^{-3/2} \exp(-|\mathbf{x}-\mathbf{y}|^2/2s)$ , reduces to

$$F(\mathbf{x}, \mathbf{y}, s, t)$$

$$= \frac{\exp(-x^2/2s - y^2/2t)}{(2\pi s)^{3/2} (2\pi t)^{3/2}} \int d\mathbf{r} \times \frac{\exp(-|\mathbf{r}|^2(1/2s + 1/2t))}{|\mathbf{r}|} \exp\left(\mathbf{r} \cdot \left(\frac{\mathbf{x}}{s} + \frac{\mathbf{y}}{t}\right)\right). \quad (A9)$$

The integral over  $\mathbf{r}$  is performed in spherical coordinates with azimuthal axis along  $\mathbf{x}/s + \mathbf{y}/t$ . This gives

$$F(\mathbf{x}, \mathbf{y}, s, t) = \frac{1}{(2\pi)^{3/2}} \frac{1}{\sqrt{s+t} |\mathbf{tx} + \mathbf{sy}|} \times \exp\left(-\frac{|\mathbf{x}-\mathbf{y}|^2}{2(s+t)}\right) \text{erf}\left(\frac{|\mathbf{tx} + \mathbf{sy}|}{\sqrt{2st(s+t)}}\right), \quad (A10)$$

where  $\text{erf}(x) = \int_0^x du e^{-u^2}$  is the error function. Thus, the square of the Hilbert-Schmidt norm of  $U_0(s)VU_0(t)V$  is

$$\begin{aligned}
& \|U_0(s)VU_0(t)V\|_2^2 \\
&= \int d\mathbf{x} \int d\mathbf{y} (F(\mathbf{x}, \mathbf{y}, s, t))^2 \frac{1}{|\mathbf{y}|^2} \\
&= \frac{\sqrt{s}}{(2\pi)^3 \sqrt{t}(s+t)} \int d\mathbf{u} \int d\mathbf{v} \\
&\quad \times \frac{e^{-|\mathbf{v}|^2}}{|\mathbf{u}|^2 |\sqrt{s}\mathbf{u} + \sqrt{t}\mathbf{v}|^2} \operatorname{erf}^2\left(\frac{|\mathbf{u}|}{\sqrt{2}}\right) \\
&\leqslant \frac{\sqrt{s}}{(2\pi)^3 \sqrt{t}(s+t)} \frac{\pi}{4} \int d\mathbf{u} \int d\mathbf{v} \frac{e^{-|\mathbf{v}|^2}}{|\mathbf{u}|^2 |\sqrt{s}\mathbf{u} + \sqrt{t}\mathbf{v}|^2} \\
&= \frac{1}{(2\pi)^3 t(s+t)} \frac{\pi}{4} \int d\mathbf{u} \int d\mathbf{v} \frac{e^{-|\mathbf{v}|^2}}{|\mathbf{u}|^2 |\mathbf{u} + \mathbf{v}|^2}. \tag{A11}
\end{aligned}$$

The second equality follows from the variable change  $\mathbf{u} = (t\mathbf{x} + s\mathbf{y})/\sqrt{st(s+t)}$ ,  $\mathbf{v} = (\mathbf{x} - \mathbf{y})/\sqrt{(s+t)}$ , while the inequality results from  $\operatorname{erf}(x) \leq \sqrt{\pi}/2$ . The last integral in Eq. (A11) is obviously finite and this gives the result of the lemma.

- <sup>1</sup>D. Langbein, *Van der Waals attraction*, Springer Tracts in Modern Physics Vol. 72 (Springer-Verlag, New York, 1974).
- <sup>2</sup>V. A. Parsegian, *Van der Waals Forces: A Handbook for Biologists, Chemists, Engineers, and Physicists* (Cambridge University Press, Cambridge, 2005).
- <sup>3</sup>L. Schiff, *Quantum Mechanics* (McGraw-Hill, New York, 1968).
- <sup>4</sup>J. Israelachvili, *Intermolecular and Surface Forces* (Academic, New York, 1995).
- <sup>5</sup>J. Mahanty and B. W. Ninham, *Dispersion Forces* (Academic, New York, 1976).
- <sup>6</sup>E. Lifchitz and L. P. Pitaevskii, *Statistical Physics Part 2*, Course of Theoretical Physics Vol. 9, edited by L. Landau and E. Lifchitz (Pergamon, New York, 1980).
- <sup>7</sup>S. A. Safran, *Statistical Thermodynamics of Surfaces, Interfaces and Membranes, Frontiers in Physics* (Addison-Wesley, Reading, MA, 1994).
- <sup>8</sup>H. I. Petracche, S. Tristram-Nagle, D. Harries, N. Kučerka, J. F. Nagle, and V. A. Parsegian, *J. Lipid Res.* **47**, 302 (2006).
- <sup>9</sup>A. Alastuey and Ph. A. Martin, *Phys. Rev. A* **40**, 6485 (1989).

<sup>10</sup>A. Alastuey, *Physica A* **263**, 271 (1999).

<sup>11</sup>D. C. Brydges and Ph. A. Martin, *J. Stat. Phys.* **96**, 1163 (1999).

<sup>12</sup>In mean-field approaches, dynamical contributions are factored out like in the classical case (Ref. 10). This amounts to wash out quantum fluctuations, so only distribution of static charges intervene in the calculation of the screened potential.

<sup>13</sup>F. Cornu and Ph. A. Martin, *Phys. Rev. A* **44**, 4893 (1991).

<sup>14</sup>A derivation of van der Waals interactions from equilibrium quantum correlations has been performed by I. Brevik and J. S. Hoye, Van der Waals forces derived from a quantum statistical mechanical path integral method, *Physica A* **153**, 420 (1988). In that work, atoms are modeled by harmonically bound charges with classical mass centers, and the screening of van der Waals forces by free charges is not considered.

<sup>15</sup>C. Fefferman, *Rev. Mat. Iberoam.* **1**, 1 (1985).

<sup>16</sup>J. G. Conlon, E. H. Lieb, and H. T. Yau, *Commun. Math. Phys.* **125**, 153 (1989).

<sup>17</sup>F. Cornu, *Phys. Rev. E* **53**, 4562 (1996); **53**, 4595 (1996).

<sup>18</sup>F. Cornu, *Phys. Rev. E* **58**, 5268 (1998).

<sup>19</sup>Ph. A. Martin, *Helv. Phys. Acta* **70**, 80 (1997).

<sup>20</sup>F. Cornu, *Phys. Rev. Lett.* **78**, 001464 (1997); *Phys. Rev. E* **58**, 5322 (1998).

<sup>21</sup>V. Ballenegger, Ph. A. Martin, and A. Alastuey, *J. Stat. Phys.* **108**, 169 (2002).

<sup>22</sup>A. Alastuey, V. Ballenegger, F. Cornu, and Ph. A. Martin, *J. Stat. Phys.* **113**, 455 (2003).

<sup>23</sup>A. Alastuey, V. Ballenegger, F. Cornu, and Ph. A. Martin, *J. Stat. Phys.* (submitted).

<sup>24</sup>A. Alastuey, F. Cornu, and Ph. A. Martin, Algebraic screening and van der Waals forces in partially ionized gases, in *Strongly Coupled Coulomb Systems*, edited by G. J. Kalman, K. Bagloev, and J. M. Rommel (Plenum, New York, 1998), p. 705.

<sup>25</sup>N. Macris and Ph. A. Martin, *J. Stat. Phys.* **60**, 619 (1990).

<sup>26</sup>The existence of  $B$  is only conjectured but not proven. All known complex entities do satisfy Eq. (2.6), which is a refined version of the H-stability condition. That inequality is essential for deriving Eq. (2.2).

<sup>27</sup>J. Ginibre, *Statistical Mechanics and Quantum Field Theory*, edited by C. DeWitt and R. Stora (Gordon and Breach, Les Houches, 1971), p. 327.

<sup>28</sup>Ph. A. Martin, *Acta Phys. Pol. B* **7**, 3629 (2003).

<sup>29</sup>Such arguments are the same as those used in Ref. 17 to establish Eq. (4.1) in the framework of prototype graphs.

<sup>30</sup>V. Ballenegger and Ph. A. Martin, *Physica A* **328**, 97 (2003).

<sup>31</sup>T. Kato, *Perturbation Theory for Linear Operators* (Springer, New York, 1966), Chap. 5, Sec. V.